Microscopic theory of the dielectric properties of proteins

Thomas Simonson,* David Perahia,‡ and Axel T. Brünger*
*The Howard Hughes Medical Institute and Department of Molecular Biophysics and Biochemistry, Yale University, New Haven, Connecticut 06511 USA; and ‡Laboratoire d'Enzymologie Physico-Chimique, Université de Paris-Sud, Orsay, France

ABSTRACT This paper investigates the microscopic mechanisms of charge screening in proteins. The screening of an arbitrary perturbing charge density by a protein and its surrounding solution is characterized by a generalized susceptibility, which is approximately given by the mean dipole–dipole correlation matrix of the system. This susceptibility is a microscopic quantity; the sum of its matrix elements gives the macroscopic susceptibility of continuum electrostatics. When screening of a single perturbing point charge is considered, this susceptibility reduces to a scalar quantity, dependent on position within the protein. The contribution of the positional degrees of freedom of the protein atoms can be estimated from molecular dynamics simulations. This contribution gives rise to large spatial variations of the susceptibility, whose significance for protein function is discussed. The model is applied to the small α helix deca-alanine, and to the electron-transfer protein cytochrome c. The results agree qualitatively with previous normal mode calculations. The importance, and the large spatial variations, of charge screening by deca-alanine suggest that dielectric screening may play a role in the binding of charged ligands by helices. In cytochrome c, the dielectric susceptibility in response to a point charge is at a minimum in the central heme region, resulting in a lowering of the reorganization free energy for charge transfer to and from the heme.

1. INTRODUCTION

In a recent article, we presented a theoretical analysis of the microscopic dielectric properties of several biomolecules (1). This analysis is pursued and refined in the present article. Our aim is to attain a better understanding of these properties at a microscopic level, and to examine the possible functional importance of the spatial variation of local dielectric properties within proteins.

Many or most enzyme reactions involve charge transfer, and the creation of a charged transition state. Several authors have analyzed theoretically the energetics of such charged transition states in various enzymes (2–9). It is now widely accepted that the efficiency of these reactions arises largely from the combination of two factors: the high polarity of the active site, and the low polarizability of this same active site (9–12). Polar groups are in effect rather rigidly preorganized around the active site to stabilize the transition state. The presence of permanent polar groups is required so that the charged intermediate species will not be destabilized in the protein compared with bulk water. Once these permanent, polar groups are given, the enzyme lowers the reorganization free energy of the charge transfer process by making these groups rather rigid. High polarity and low polarizability thus combine to give enzyme active sites electrostatic and dielectric properties that are both complex and specific. This specificity led Simonson et al. (1) to suggest that the spatial variation of local dielectric properties in proteins may have functional significance. For example, by providing a polarizability at the active site that is lower than in the rest of the molecule, an enzyme would achieve an additional lowering of its reorganization free energy, beyond what is provided by the average dielectric properties of the molecule. Obviously, the local polarizability around the reactants is already lowered considerably simply by the removal of the active site from bulk water, since the protein is less polarizable than water. In fact, the solvent polarization ordinarily makes the dominant contribution to the reorganization free energy for the charge transfer steps (2). However, the protein contribution is not negligible, and presumably needs to be minimized by the enzyme. This can be accomplished by reducing the electronic polarizability around the active site, and by making the permanent, preorganized polar groups as rigid as possible, given the other due requirements of the structure, such as sufficient flexibility to sterically accommodate the reactants.

Enzyme active sites are not the only examples of specific local dielectric properties in proteins. The binding of charged ligands requires that the protein "solvate" these ligands as effectively as water. This can of course be accomplished by the presence of permanent, preordered, charged, or dipolar groups, as in active sites. However, where binding, not reaction kinetics, is important, it may be more economical for a protein to adjust

0006-3495/91/03/670/21 $2.00

its local structure solely in response to the approach of the ligand, rather than paying the cost of preorganized dipoles. In other words, it may be more economical to provide a less polar, but more polarizable, binding site.

To investigate electrostatic and dielectric properties of proteins, the simplest model is the continuum model (13). Early continuum treatments of proteins included as permanent charges only ionized side chains (14), and in some cases the macrodipoles of α helices (15). This treatment of course neglects precisely the permanent polar groups required to stabilize enzyme transition states (16). Subsequent continuum models did include these groups (17), and could in principle address the energetics of enzyme transition states. A low protein dielectric constant of around four is usually used, and is designed to describe both electronic polarizability and dipolar polarizability; the latter includes elastic deformation of bonds and angles, and rotation of polar groups around bonds. The exact significance of the protein dielectric constant ϵ_p clearly changes when the permanent charges in the model change. Indeed, the dielectric constant enters into the model in two ways. It determines the response of the system to a set of perturbing charges, such as a titrating proton or a redox electron. But it also determines the mean equilibrium charge distribution. For example, suppose the model includes as permanent charges only point charges representing the ionized side chains (e.g., references 14 and 15). The mean equilibrium charge distribution will then include not only these charges, but also induced polarization charge located on the permanent charges, and induced surface charge distributed all over the protein-solvent interface. To be precise, the permanent charges will be divided by a factor ϵ_p. The polarization charge on the permanent charges represents the screening (e.g., by hydrogen-bonding) provided by the polar groups of the protein not included in the model as permanent charges. (Note a potential inconsistency of most implementations of the model: the fact that for most ionized side chains, this screening is mainly coming from water molecules, so that it would appear more consistent to assign these side chains to the high-dielectric region, as in reference 18.) Now adopt a model with the same protein dielectric constant ϵ_p, but which includes as permanent charges the mean partial atomic charges of all the protein atoms (e.g., reference 17), including the net charges of the ionized side chains (which are now spread over the whole side chain). Although the dielectric polarization of this model in response to a set of perturbing charges will be identical to the previous model, it will have a completely different mean equilibrium charge distribution. In other words, a completely different description will be given of the way in which each group of charges is polarized by neighboring groups, once these groups are folded together in the protein.

In describing the response of the folded protein to a perturbation, the low dielectric constants used are compatible with dielectric measurements on protein powders (19–22). These measurements tell us about spatially averaged dielectric properties; they tell us little about specific local properties, for example, around an active site. Similarly, a continuum model that uses a uniform, scalar, dielectric constant cannot account for specific dielectric properties around an active site.

A low ϵ_p is also compatible with theoretical estimates, based on the theory of dielectrics (23–25, 1). These estimates use atomic point polarizabilities to describe electronic polarizability, and molecular dynamics simulations to describe dipolar polarizability. They can be applied not only to an entire protein, but also to a local region in a protein. Nakamura et al. (25), for example, calculated the dielectric constant within a sphere of 4–8 Å radius, whose position was varied throughout the protein. This defines a position-dependent dielectric constant, which reflects the local electronic polarizability and molecular dynamics within the sphere. For our purposes, this approach has two serious limitations. First, though it does give a local dielectric constant, this quantity is a spatial and a rotational average over a region of several Angstroms radius. This averaging may smooth out significant local details, especially if the region of spherical averaging is taken to be large. In the simulations presented in our previous paper for example, and those presented below, large spatial variations of the local dielectric susceptibility are found in several biomolecules, over distances of only a few Angstroms. Second and more important, this approach views the region outside the sphere as a featureless dielectric continuum. This is the Onsager approximation (26), clearly a serious one in proteins, unless the sphere considered is quite large.

We see that although a continuum model can indeed address the energetics of enzyme catalysis, and even take into account nonuniform dielectric properties in proteins to an extent, this approach is not the method of choice to examine our working hypothesis. Indeed, though Krishtalik has used a continuum model to analyze a number of charge transfer reactions in a model spherical enzyme (9), all studies of real enzymes have been based on detailed microscopic models (5–8). Many of these analyses have used the perturbation free energy technique. This is computationally very expensive, in contrast to continuum models. We adopt instead a microscopic approach whose complexity is intermediate between macroscopic models and complete perturbation free energy calculations. This approach combines elementary linear response theory with techniques of

free energy calculation. To characterize the local dielectric properties of a protein, we introduce the generalized susceptibility of the molecule in response to a static, perturbing, charge density. This generalized susceptibility is an operator in a $3n$-dimensional space, where n is the number of atoms in the system. The sum of its elements is equal to the macroscopic susceptibility of continuum electrostatics (13). Unlike the macroscopic susceptibility, which is a spatial average, and which describes in effect the response to a slowly-varying (i.e., long-wavelength) field, the generalized susceptibility is a microscopic quantity, which describes the response to an arbitrary field. To calculate this susceptibility, we use a simple, standard, model of the electronic and positional degrees of freedom of the molecule. The electronic degrees of freedom are approximated by atomic point polarizabilities. The positional degrees of freedom of the atoms are described by molecular dynamics. Our previous article considered a perturbing charge density made up of a sole point charge. In the present article we generalize this approach to an arbitrary perturbing charge density.

In the applications described previously, the normal mode approximation was used to simulate the protein dynamics. An analytical expression of the susceptibility was obtained, valid within this approximation. The normal mode approximation makes the analysis simple, elegant, and very inexpensive. The normal modes are expected to usefully approximate the dynamics of the molecule over fairly short time segments, on the order of ten picoseconds. At the same time, this description has obvious limitations. One of the most important is its incapacity to deal with the dynamics of the surrounding solvent. It is thus necessary to carry out simulations using full molecular dynamics. This paper will therefore extend the previous theory and simulations to the general, anharmonic, case.

To a first approximation, it appears reasonable to distinguish the dielectric relaxation of the protein from that of the solvent, and to assume that they can be calculated separately. This assumption was made in our previous study, as well as in some work by other authors (e.g., reference 3). It will be made here as well. As a first step, we therefore investigate several biomolecules in artificial, vacuum, conditions. It is crucial to go beyond this first approximation and to investigate not only the relative importance of protein and solvent relaxation, but also the coupling between the two effects. This analysis is underway and will be presented in a separate article.

As model systems to illustrate and test our approach, we previously chose the model α helix deca-alanine, several α helices extracted from various proteins, and the electron transfer protein cytochrome *c*. In this study, deca-alanine and cytochrome *c* are used.

This article therefore pursues the development of a microscopic theory of the dielectric properties of proteins, initiated in our previous study. The calculations presented below address several important aspects of this theory. The first aspect addressed is the general behavior of the local dielectric properties throughout a protein. Specifically, we investigate several properties of the susceptibility: its average value, its spatial nonuniformity, the relative importance of electronic and dipolar relaxation, the importance of dielectric saturation, as well as other properties. A second aspect addressed is the significance of the susceptibility's spatial variation for biological function, in other words, our working hypothesis. A third aspect, the relative magnitude of the protein and solvent relaxation, and the coupling between the two, will be addressed in a future paper.

This paper is organized as follows. In the second section the calculation of the susceptibility is presented. In particular, the analytical expression of the dipolar susceptibility, previously obtained in the harmonic case, is extended to the anharmonic case, within the limit of small fluctuations. The methodology of the simulations is also described. In the third section the results are presented. They are discussed in the final section.

2. MATERIALS AND METHODS

Definition of the microscopic susceptibility

Consider a set of nondiffusive charges such as a folded protein. To characterize the dielectric properties of this system microscopically (1), we introduce a fixed, perturbing, charge density ρ, which produces a perturbing field $\underline{f}$. The perturbing Hamiltonian V_{tot} contains a "static" term V_{static} and a relaxation term V:

$$V_{tot} = V_{static} + V. \tag{1}$$

The first term is associated with introducing the perturbation while constraining the system to retain its unperturbed structure. The second term is associated with the relaxation after the constraints are removed. In the limit where the perturbation is vanishingly small, the relaxation energy is proportional to the perturbing field:

$$V = -\underline{x} \cdot \underline{f}. \tag{2}$$

$\underline{f}$ denotes the $3n$-vector:

$$\underline{f} = (\underline{f}_1, \underline{f}_2, \ldots, \underline{f}_n), \tag{3}$$

where $\underline{f}_i$ is the field of the test charge at the *mean* position of atom i, and n is the number of atoms in the system. The conjugate quantity $\underline{x}$ is also a $3n$-vector, which represents the structural relaxation of the

system. The "discrete" form of V results from the nondiffusive nature of the system.

The relaxation can be characterized by a generalized susceptibility $\hat{\alpha}$, which is a linear operator (e.g., reference 27). By definition

$$\langle \underline{x} \rangle = \hat{\alpha} \underline{f}. \tag{4}$$

The brackets represent an ensemble average. The matrix elements of the susceptibility are related to the components of $\underline{x}$ by the fluctuation-dissipation theorem (28):

$$\hat{\alpha}_{mn} = \frac{1}{kT} \langle x_m x_n \rangle_0. \tag{5}$$

The brackets $\langle \rangle_0$ represent an ensemble average over the phase space of the unperturbed molecule. The susceptibility and the associated dielectric relaxation are thus completely determined by the fluctuations of the unperturbed system. The ensemble average of the relaxation energy can be written

$$\langle V \rangle = -\underline{f} \cdot (\hat{\alpha} \underline{f}). \tag{6}$$

Like V_{tot}, the total perturbation free energy A_{tot} has a static component A_{static} and a relaxation component A. The static component is just the ensemble average of V_{tot} in the absence of the perturbation. Thus:

$$A_{tot} = \langle V_{tot} \rangle_0 + A. \tag{7}$$

The relaxation free energy A has the general form

$$A = -kT \ln [\langle \exp(-V_{tot}/kT) \rangle_0] - \langle V_{tot} \rangle_0. \tag{8}$$

For the vanishingly small perturbation considered here, this expression can be expanded into:

$$A = -\frac{1}{2kT} (\langle V_{tot}^2 \rangle_0 - \langle V_{tot} \rangle_0^2). \tag{9}$$

To express A as a function of the susceptibility, let us consider a process where the perturbation is introduced gradually. During this process, the perturbing charge density is $\lambda\rho$, the perturbing field is $\lambda \underline{f}$, and λ is varied from zero to one. Incrementing λ by $d\lambda$ changes the relaxation free energy by

$$dA = \frac{dA}{d\lambda} d\lambda = \left\langle \frac{\partial V}{\partial \lambda} \right\rangle_\lambda d\lambda = -\langle \underline{x} \rangle_\lambda \cdot \underline{f}\, d\lambda = -\lambda \underline{f} \cdot (\hat{\alpha} \underline{f})\, d\lambda. \tag{10}$$

The brackets $\langle \rangle_\lambda$ indicate an average over the phase space of the system in the presence of the intermediate charge density $\lambda\rho$. Integrating from $\lambda = 0$ to $\lambda = 1$ gives

$$A = -\tfrac{1}{2} \underline{f} \cdot (\hat{\alpha} \underline{f}). \tag{11}$$

The susceptibility operator is an intrinsic property of the system, which does not depend on the particular perturbing charge density being considered. It gives a complete description of the dielectric properties of the system. In particular, it determines the macroscopic dielectric properties of the system, such as its dielectric constant. To see this, consider a large, macroscopically homogeneous, isotropic system, and apply a uniform external field $\underline{e}$. The relaxation free energy of this system in response to $\underline{e}$ is

$$A = -\tfrac{1}{2} \underline{E} \cdot (\hat{\alpha} \underline{E}), \tag{12}$$

where $\underline{E} = (\underline{e}, \underline{e}, \ldots, \underline{e})$ is a $3n$-vector. Rearranging this product and using the isotropic nature of the system, we find

$$A = -\frac{1}{2} \sum_{mn} \alpha_{mn} e^2. \tag{13}$$

If the system is a sphere of radius R surrounded by a vacuum, A can be calculated from electrostatics (30) as a function of the dielectric constant ϵ of the system; we obtain

$$\frac{\epsilon - 1}{\epsilon + 2} = \frac{1}{R^3} \sum_{mn} \alpha_{mn}. \tag{14}$$

The double sum is over all the atoms of the system, i.e., it represents a spatial average. Thus the macroscopic dielectric constant, or the macroscopic susceptibility $(\epsilon - 1)/4\pi$, in effect measures the response of the system to a perturbing field that varies *slowly* with respect to the separation between atoms. In contrast, the generalized susceptibility $\hat{\alpha}$ determines the relaxation in response to a small, but otherwise *arbitrary,* perturbing charge distribution.

In the next section, we shall derive the explicit expression of the full susceptibility operator for a system undergoing small, nondiffusive, fluctuations. However, it will also be useful to introduce a related but simpler parameter, which gives a partial characterization of the dielectric response of the system. Let us define the scalar quantity α by the equality:

$$A = -\tfrac{1}{2} \underline{f} \cdot (\alpha \underline{f}) = -\tfrac{1}{2} \alpha \underline{f}^2. \tag{15}$$

Strictly speaking, α is the projection of the operator $\hat{\alpha}$ onto a certain one-dimensional subspace. By construction, α contains precisely all the information necessary to characterize the relaxation free energy of the system in response to ρ. Therefore, we may refer to α as an "effective scalar susceptibility." Unlike $\hat{\alpha}$, the scalar susceptibility is a function of ρ. For example, if ρ is made up of a single perturbing point charge, then α is a function of the position of this charge. In what follows, when we speak of the susceptibility we shall frequently be referring not to the complete susceptibility operator $\hat{\alpha}$, but to its most useful part, the projection α.

Expression of the susceptibility for a nondiffusive system

The relaxation free energy and the susceptibility $\hat{\alpha}$ are determined by the fluctuations of the unperturbed system. As a result, very simple, analytical expressions can be obtained for these quantities. Let us first assume that the perturbing charge density ρ is made up of a single point charge q. The Coulomb interaction V_{tot} between the perturbing charge and the protein can be expanded as a power series of the variables u_i/r_{iq}, where $\underline{r}_{iq}$ is the vector joining the mean position of atom i to the test charge q, and $\underline{u}_i$ is the instantaneous displacement of atom i from its mean position. Inserting this expansion into Eq. 9 and neglecting terms of order four or more, the relaxation free energy takes the form:

$$A \approx -\frac{q^2}{2kT} \sum_{i,j} \frac{q_i q_j}{r_{iq}^3 r_{jq}^3} \langle (\underline{u}_i \cdot \underline{r}_{iq})\, (\underline{u}_j \cdot \underline{r}_{jq}) \rangle_0. \tag{16}$$

The first- and third-order term have vanished by symmetry. The summation is over all pairs of atoms i, j. This expression is valid in the limit of small fluctuations. Denoting r^x (respectively r^y, r^z) the component of a vector $\underline{r}$ along x (respectively y, z), we have:

$$A \approx -\frac{q^2}{2kT}\sum_{i,j}\frac{q_i q_j}{r_{iq}^3 r_{jq}^3}\sum_{\alpha,\beta\in\{x,y,z\}} r_{iq}^{\alpha} r_{jq}^{\beta}\langle u_i^{\alpha} u_j^{\beta}\rangle_0. \tag{17}$$

Let us introduce the mean correlation matrix **M** of the instantaneous atomic dipoles, defined by:

$$M_{i\alpha,j\beta} = q_i q_j \langle u_i^{\alpha} u_j^{\beta}\rangle_0. \tag{18}$$

We see that the expression Eq. 17 of the relaxation free energy can be rewritten in a very simple matrix form: A is none other than

$$A \approx -\frac{1}{2kT}\underline{f}\cdot(\mathbf{M}\underline{f}). \tag{19}$$

This is the approximate relaxation free energy of an arbitrary set of nondiffusive charges (such as a protein) in response to a vanishingly small, static point charge q. It depends on the fluctuations of the unperturbed set of charges through the matrix **M**, and on the position and magnitude of the perturbing charge through the vector $\underline{f}$. The derivation assumes that the fluctuations of the atoms are small with respect to the atoms' distance from the perturbing charge, i.e., it is valid in the limit of small atomic fluctuations. For a folded protein, with a well-defined average structure, this should in many cases be a weak assumption.

The preceding expression of the relaxation free energy can be immediately generalized to an arbitrary set of perturbing charges. Consider two such charges, q_1 and q_2. The relaxation free energy A can be written (with obvious notations):

$$A = -\frac{1}{2kT}(\langle V_1^2\rangle_0 - \langle V_1\rangle_0^2) - \frac{1}{2kT}(\langle V_2^2\rangle_0 - \langle V_2\rangle_0^2)$$

$$-\frac{1}{kT}(\langle V_1 V_2\rangle_0 - \langle V_1\rangle_0\langle V_2\rangle_0). \tag{20}$$

Let r_{i1} and r_{i2} be the distances from the mean position of atom i to the charges 1 and 2. $\langle V_1 V_2\rangle_0$ can be expanded with respect to the quantities u_i/r_{i1} and u_i/r_{i2}, just as $\langle V_{tot}^2\rangle_0$ was expanded earlier with respect to u_i/r_{iq}. The calculation is virtually identical, and leads to

$$\langle V_1 V_2\rangle_0 - \langle V_1\rangle_0\langle V_2\rangle_0 \approx q_1 q_2 \sum_{i,j}\frac{q_i q_j}{r_{i1}^3 r_{j2}^3}\sum_{\alpha,\beta\in\{x,y,z\}} r_{i1}^{\alpha} r_{j2}^{\beta}\langle u_i^{\alpha} u_j^{\beta}\rangle_0 \tag{21}$$

$$\approx \underline{f}_1\cdot(\mathbf{M}\underline{f}_2). \tag{22}$$

$\underline{f}_a$ denotes $\underline{f}\,(q = q_a)$. We obtain finally:

$$A \approx -\frac{1}{2kT}(\underline{f}_1 + \underline{f}_2)\cdot\mathbf{M}(\underline{f}_1 + \underline{f}_2). \tag{23}$$

The cross-wise term $\underline{f}_1\cdot(\mathbf{M}\underline{f}_2)$ represents the coupling between the polarization induced by q_1 and that induced by q_2.

Clearly, the analogous formula holds for a set of p perturbing point charges:

$$A \approx -\frac{1}{2kT}\underline{f}_{tot}\cdot(\mathbf{M}\underline{f}_{tot}), \tag{24}$$

where

$$\underline{f}_{tot} = \sum_{a=1}^{p}\underline{f}_a. \tag{25}$$

An arbitrary perturbing charge density ρ can be expressed as an infinitesimal sum of point charges. Therefore the relaxation free energy again takes the form

$$A \approx -\frac{1}{2kT}\underline{f}(\rho)\cdot[\mathbf{M}\underline{f}(\rho)]. \tag{26}$$

Comparing Eqs. 11 and 26, we see that the susceptibility operator $\hat{\alpha}$ is approximately equal to the dipole–dipole correlation matrix **M** divided by kT:

$$\hat{\alpha} \approx \frac{1}{kT}\mathbf{M}. \tag{27}$$

This expression is valid for a nondiffusive system, in the limit of small u_i/r_{iq}; it will be convenient to speak of the "small-fluctuation" limit.

The existence of a relationship between the dielectric properties and the microscopic correlations of atomic positions is a well-known and general property of polar media. It was first pointed out by Kirkwood (29) and Fröhlich (30) in the case of polar, nonpolarizable, fluids. Their theory has been extended to more complex fluids by a large number of authors (31, 32). In particular, fluids containing free ions have been analyzed (e.g., 31, 33, 34). Our analysis focuses on nondiffusive systems. The analytical, small-fluctuation form of the susceptibility has several consequences that should be noted here. First, if the "protein" contains only a single charge q_1, and if the perturbation ρ is made up of a single point charge q, then

$$A \approx -\frac{q^2}{r_{1q}^4}\frac{q_1^2\langle(u_1^x)^2\rangle_0}{2kT}, \tag{28}$$

where x is the axis joining the protein charge to the perturbing charge. The corresponding susceptibility is

$$\alpha \approx \frac{q_1^2\langle(u_1^x)^2\rangle_0}{kT}. \tag{29}$$

The protein-perturbing charge distance does not enter into α. The susceptibility is determined by the fluctuations of the unique protein atom along the protein charge-test charge axis. The reason for this is clear. When the test charge is introduced, the "protein" relaxation is simply a motion of the protein charge toward or away from the test charge. The amplitude of this relaxation is directly reflected by the softness of the unperturbed fluctuations along this direction. This result is accurate to the fourth order with respect to

$$[\langle(u_1^x)^2\rangle_0]^{1/2}/r_{1q}.$$

To a higher accuracy, fluctuations of the protein charge along the other two spatial directions also make small contributions to the susceptibility. In general, we expect that soft fluctuations of polar groups will give rise to large local susceptibilities, because these groups can move extensively along their soft degrees of freedom in response to a perturbation.

Second, if we compare the expressions 5 and 18 of $\hat{\alpha}$ and **M**, we see that the conjugate quantity $\underline{x}$ is given (in the small-fluctuation limit) by

$$x_{i\alpha} = q_i u_{i\alpha}. \tag{30}$$

In the small-fluctuation limit, $\underline{x}$ is given by the list of the instantaneous dipoles on each atom. When $\underline{f}$ is applied, the average of these instantaneous dipoles becomes nonzero, and proportional to $\underline{f}$.

The analytical form of the susceptibility has a third consequence, which concerns the quasiharmonic description of the protein dynamics (35). In the quasiharmonic approximation, the protein is assumed to be vibrating along a set of quasinormal modes. These are obtained by diagonalizing the displacement correlation matrix σ, defined by:

$$\sigma_{i\alpha,j\beta} = \langle u_i^\alpha u_j^\beta \rangle. \tag{31}$$

Thus the quasiharmonic approximation is designed to preserve the correlations of the atomic displacements. As a result, the quasiharmonic approximation also preserves the dipole correlation matrix **M**. In other words, in the limit where the atomic fluctuations are small, the quasiharmonic approximation leads to *exactly the same* dielectric properties as the full molecular dynamics model.

Finally, in the harmonic approximation, we have the relationship

$$\langle u_i^\alpha u_j^\beta \rangle_0 \propto kT. \tag{32}$$

Thus

$$\mathbf{M} \propto kT, \tag{33}$$

and the susceptibility operator $\hat{\alpha}$ is independent of the temperature. In other words, the temperature dependence of the dielectric properties is an effect of the anharmonicity of atomic motions. If the system becomes frozen into a local energy minimum at low temperature, its vibrations will become roughly harmonic, and the reorganization free energy for charge transfer should become roughly independent of the temperature (provided quantum corrections are not important). This has implications for the kinetics of electron-transfer proteins.

Dielectric saturation

Our formalism also provides a way to directly predict dielectric saturation effects in biomolecules. Consider the perturbation free energy due to a finite perturbing charge q. We can expand this free energy as a power series of the perturbing potential V_{tot}. For a vanishing perturbing charge, the relaxation free energy is just the second order term, given in Eq. 9, proportional to q^2. For a finite perturbing charge, the third- and higher-order terms produce a deviation from this behavior, which is to be interpreted as the effect of dielectric saturation. To calculate this effect, we calculate the complete relaxation free energy, which has the general form:

$$A(q) = -kT\ln[\langle \exp(-V_{tot}/kT)\rangle_0] - \langle V_{tot}\rangle_0. \tag{34}$$

The difference between $A(q)$ and the second-order term measures dielectric saturation. Dividing $A(q)$ by the square of the field f of the charge, we obtain a quantity $\alpha_{eff}(q)$. By analogy to the expression 15 of A, we can view $\alpha_{eff}(q)$ as an effective susceptibility:

$$A(q) = -\frac{1}{2} f \cdot [\alpha_{eff}(q) f]. \tag{35}$$

This effective susceptibility provides an equivalent, and slightly more convenient, measure of the dielectric saturation.

Fröhlich-Kirkwood dielectric constant of a protein

The analysis based on the generalized susceptibility gives a purely microscopic description of the protein's dielectric behavior. It is of interest to complement this analysis with a simpler, independent analysis, based on a macroscopic model. Let us therefore view the protein momentarily as a macroscopic system, and estimate its dielectric constant from Fröhlich-Kirkwood theory (30). This dielectric constant is a simple indicator of the average dielectric properties of the molecule. Such an estimate (24, 25, 1) can be compared with dielectric measurements on protein powders, and to the empirical dielectric constants used in continuum models of the Tanford-Kirkwood type. We treat the protein as a macroscopic sphere of radius R. Assigning a point polarizability α_i to each atom i, the high-frequency dielectric constant is obtained from the Clausius-Mossotti equation:

$$\frac{\epsilon_\infty - 1}{\epsilon_\infty + 2} = \frac{\alpha_{tot}}{R^3}. \tag{36}$$

The total electronic polarizability α_{tot} is approximately equal to the sum of the individual atomic polarizabilities:

$$\alpha_{tot} \approx \sum_i \alpha_i. \tag{37}$$

The difference is of order two with respect to the dipole-dipole tensor of the protein (1). The overall dielectric constant can then be related to the instantaneous dipole moment M_{dip}, which arises from the reorientation of permanently polarized groups such as the peptide bond. Two situations can arise. If the protein is embedded in an infinite medium that has the same dielectric constant as itself, then Fröhlich's relation applies:

$$\frac{(2\epsilon + \epsilon_\infty)(\epsilon - \epsilon_\infty}{3\epsilon} = \frac{\langle M_{dip}^2 \rangle}{kTR^3}. \tag{38}$$

If the protein is surrounded by a vacuum, then an analogous relation, derived by Simonson et al. (1), applies:

$$\frac{\epsilon - \epsilon_\infty}{\epsilon + 2} = \frac{\langle M_{dip}^2 \rangle}{3kTR^3}. \tag{39}$$

$\langle\,\rangle$ represents a Boltzmann average over the spontaneous fluctuations of M_{dip} in the absence of applied field.

Methodology of the simulations

The calculations presented below were done using the program X-PLOR (36). The susceptibility can be calculated using either the exact expression (9) of the relaxation free energy, or using the small-fluctuation form (19). The latter form assumes the test charge is not too close to the protein atoms. Because the atomic displacement correlation matrix is available in X-PLOR and other molecular dynamics packages, it is straightforward to implement the expression (19) in these packages. This method is considerably faster than the use of the exact expression (9). The two methods will be compared below.

The model systems considered here are deca-alanine and cytochrome *c*. Rather than rely on the normal mode approximation, full molecular dynamics simulations were performed. As previously, the model includes all atoms explicitly, except for *CH*, CH_2, and CH_3 groups, which are treated as extended atoms. Hydrogen bonding is described purely in terms of electrostatic interactions, and the model does not include many-body induction forces. The Charmm/Param19 force field was used (37). The simulations were performed *in vacuo*.

In the case of deca-alanine, the *N*-terminus was blocked by a CH_3—*CO* group, and the *C*-terminus was blocked by an *NH*—CH_3 group. The starting structure was obtained by building an idealized helix, then doing energy minimization. Four separate simulations were

done, including a total of 40 ps of equilibration and 150 ps of data collection. Newton's equations of motion were integrated using a timestep of one femtosecond. Bonds to hydrogen atoms were constrained with the algorithm SHAKE (38). Coupling to a 298 K temperature bath was performed using the method of Berendsen et al. (39), with a characteristic coupling time of 0.1 ps. No cutoff was used for nonbonded interactions. The overall rotation translation of the molecule, which arises from small errors in the integration, was removed by least-squares fitting the instantaneous structure to a reference structure.

In the case of cytochrome *c*, the starting structure was the x-ray structure of tuna ferricytochrome *c* (40). Bond constraints, temperature coupling, and time step were the same as for deca-alanine. Electrostatic interactions were shifted to zero at a cutoff distance of 12 Å. Random initial velocities were assigned, and 30 ps of equilibration performed, followed by 90 ps of data collection. Since the simulations were done *in vacuo*, there are in effect no long-range forces in the system. Therefore truncation of the electrostatic forces beyond 12 Å should be a minor approximation. If a protein in solution were considered, a continuum correction would be necessary to compensate for such truncation. In the case of spherical truncation, for example, the continuum correction to the free energy of a point charge is the well-known Born energy.

In the cytochrome *c* calculations, a perturbing test charge was actually placed on atoms within the protein. Atoms separated by one or two bonds from the test charge were excluded from the perturbation potential.

In the calculations of the Fröhlich-Kirkwood dielectric constants, the radius R was taken to be the radius of the sphere with the same radius of gyration as the protein. The polarizabilities α_i were set to 1 Å^3 for heavy atoms and 0.5 Å^3 for hydrogen atoms.

3. DECA-ALANINE RESULTS

Structure and fluctuations of deca-alanine

The r.m.s. atomic fluctuations during the 150 ps of molecular dynamics simulation are described in Tables 1 and 2, and Fig. 1. The results for the oxygen and amide hydrogen atoms are given apart, as they make the largest contribution to the susceptibilities. The results of the normal mode calculation are given for comparison. The average molecular dynamics fluctuation is 0.61 Å, including all atoms. The harmonic result was 0.35 Å. The larger motion of the helix termini, illustrated in Fig. 1, does not occur in the harmonic approximation. The mean, simulated structure deviates from the initial, energy minimum structure by 0.25 Å, and the structure shows no systematic drift during the simulation.

TABLE 1 Average r.m.s. atomic fluctuations in deca-alanine

	All atoms	Backbone	Oxygens and amide hydrogens
Normal modes	0.35	0.30	0.41
Molecular dynamics	0.61	0.57	0.64

Rms fluctuations (Å) of deca-alanine atomic positions, calculated from molecular dynamics and from the harmonic approximation.

TABLE 2 R.m.s. atomic fluctuations in deca-alanine

Residue number	All atoms	Backbone	Oxygens, amide hydrogens	Oxygens, amide hydrogens, harmonic approximation
1	1.28	1.36	1.11	0.32
2	0.90	0.76	1.06	0.40
3	0.49	0.41	0.53	0.39
4	0.39	0.34	0.39	0.37
5	0.39	0.34	0.43	0.37
6	0.41	0.36	0.42	0.36
7	0.42	0.37	0.46	0.36
8	0.41	0.36	0.44	0.39
9	0.48	0.42	0.53	0.43
10	0.60	0.51	0.65	0.44
11	0.83	0.70	0.92	0.45
12	1.47	1.54	1.34	0.40

Root mean square fluctuations (Å) of atomic positions, averaged over each residue of the helix (counting the two terminal blocking groups $CH_3 - CO$ and $NH - CH_3$ as residues 1 and 12, respectively).

Fröhlich-Kirkwood dielectric constant of deca-alanine

Before analyzing the microscopic dielectric properties of the deca-alanine, it is instructive to view the molecule as a macroscopic dielectric body, and to estimate its overall dielectric constant from Fröhlich-Kirkwood theory (30), as described in Materials and Methods. The high-frequency dielectric constant ϵ_∞ was previously estimated to be 1.7 (1). The effective molecular "radius" is 7

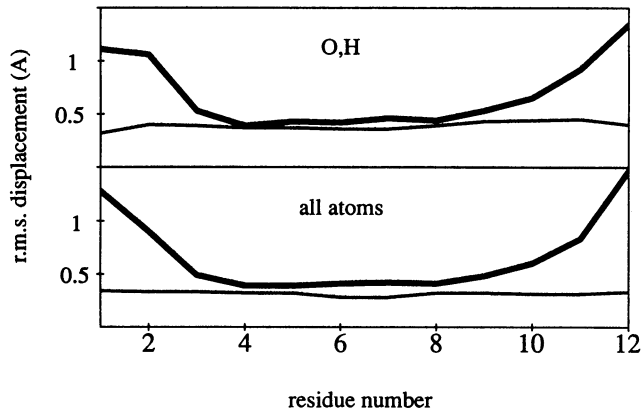

FIGURE 1 R.m.s. atomic fluctuations in deca-alanine, averaged over the individual residues, as a function of residue number. Results for all atoms (*lower curves*) and for the oxygen and amide hydrogen atoms (*upper curves*). Molecular dynamics result (*bold*); harmonic result (*light*). Residues 1 and 12 designate the two terminal groups, $CH_3 - NH$ and $CO - CH_3$.

Å. The total dielectric constant is then estimated from the simulation to be 3.3, using the *in vacuo* expression (Eq. 39) of ϵ. The harmonic value was 2.3 (Table 3). The larger molecular dynamics fluctuations are responsible for the larger dielectric constant. Obviously, deca-alanine is not really a macroscopic, spherical, dielectric medium, so these values are merely rough indicators of its dielectric behavior. As such, both of these results are compatible with experimental observations of protein powders, as well as with empirical values commonly used in macroscopic models (23). Note that if the "infinite medium" expression (Eq. 38) of ϵ were used, we would obtain a rather different value of $\epsilon = 2.8$. Therefore it is indeed important, if deriving the dielectric constant from a vacuum simulation, to use the Fröhlich-type relation that is actually adapted to a vacuum situation.

Dielectric behavior of deca-alanine

To probe the microscopic dielectric properties of the molecule we introduce a perturbing point test charge. To study the variation of the susceptibility over the surface of the molecule, we consider the solvent-accessible surface of the molecule. Because α helices in proteins frequently interact with charged ligands located 2–4 Å away, a second surface is derived by translating the solvent-accessible surface 4 Å away from the molecule, along the local normal to the surface. This 4 Å surface was approximated by a discrete dot-surface using the program MS of Connolly (41). The test charge's position was varied over this discrete dot-surface. Surface maps of all the relevant quantities were thus obtained. A vanishingly small test charge was considered, as in our previous, harmonic calculations. Two finite test charges, $q = 1$ atomic unit and $q = ¼$ atomic unit, were also considered, to estimate the importance of dielectric saturation. "Exact" calculations (based on the exact expression 9) were done using a 60-ps segment of the trajectory. Unless specified, the results presented below are derived from this exact calculation. Approximate calculations, based on the analytical, small-fluctuation expression (19) were also done, using the entire 150 ps trajectory.

The perturbation free energy A_{tot} has a static component, A_{static}, and a relaxation component, A (Eq. 7). The first term is just the interaction of the test charge with the mean, unperturbed structure: $A_{static} = \langle V_{tot} \rangle_0$. The second term determines the susceptibility: $A = -\alpha f^2$. The averages of the different energy terms over the surface map are given in Table 4. These terms include A_{static}, A, and the electronic relaxation free energy (from reference 1) A_{elec}. The average of the absolute magnitude $|A_{static}|$ is also given. These all refer to a vanishingly small test charge, by construction, and they are all in kcal/mol/e units; i.e., they are normalized to a unit charge, for convenience. The analogous free energy terms are given for the finite charges $q = ¼$ au and $q = 1$ au. The averages of the susceptibility α, the two effective susceptibilities $\alpha_{eff}(q = ¼)$ and $\alpha_{eff}(q = 1)$, and the electronic susceptibility α_{elec} are given as well. The variances of all these quantities over the surface map are shown in parentheses, to give an idea of the spatial nonuniformity of the dielectric properties. (Note that these are spatial variances, and *not* estimates of the statistical errors.) The average of α is 1.77 Å^3. The harmonic result was 1.58 Å^3. (The slightly different result given by Simonson et al. [1] is an average over both the 4-Å surface and the analogous 2-Å surface.) The average of $\alpha_{eff}(q = ¼)$ is 1.88 Å^3; the average of $\alpha_{eff}(q = 1)$ is 1.72 Å^3. Note that the difference between α and $\alpha_{eff}(q = ¼, 1)$ is a direct measure of dielectric saturation. Note also that the average electronic susceptibility was previously found to be 0.92 Å^3. For a negative test charge in the region of positive molecular potential, around the *N*-terminal half of the molecule, $A_{static} = -|A_{static}| \approx -9.2$ kcal/mol/e. Therefore the total interaction free energy of the test charge with the helix is about $-9.2 - 2.8 - 1.8 = -13.8$ kcal/mol/e. For points close to the *N*-terminus, the free

TABLE 3 Fröhlich-Kirkwood dielectric constant of deca-alanine

	ϵ	ϵ_∞
Harmonic approximation	2.3	1.7
Molecular dynamics	3.6	1.7

Dielectric constant of deca-alanine estimated from the molecular dynamics and normal mode simulations.

TABLE 4 Susceptibilities averaged over 4 Å surface of deca-alanine

	Molecular dynamics	Normal modes
α	1.77 (1.33)	1.58 (0.94)
$\alpha_{eff}(q = ¼)$	1.88 (1.80)	—
$\alpha_{eff}(q = 1)$	1.72 (1.54)	—
α_{elec}	0.92 (0.04)	—
A_{static}	2.1 (10.6)	—
$\lvert A_{static} \rvert$	9.2 (5.5)	—
$A(q \to 0)$	−2.8 (2.4)	−3.0 (1.6)
$A(q = ¼)$	−3.1 (3.3)	—
$A(q = 1)$	−2.7 (2.0)	—
A_{elec}	−1.8 (0.6)	—

Dielectric susceptibilities (Å^3) and relaxation free energies of deca-alanine averaged over surface map. The variances over the surface map are given in parentheses. Molecular dynamics and normal mode results. The electronic component α_{elec} is also shown. The relaxation free energies are given in kcal/mol/e; i.e., they are normalized to a unit charge.

energy is much lower: subtracting two standard deviations of A_{static} and A, we get $-13.8 - 11.0 - 4.8 = -29.6$ kcal/mol/e. 25% of this number is relaxation free energy. These numbers correspond to charges 4 Å away from the helix.

To permit a simple representation of the susceptibility's spatial variation, the susceptibility maps were averaged over the surface of each residue of the helix. Fig. 2 shows the susceptibility as a function of residue number. The result of a normal mode calculation is given as well as the molecular dynamics result.

Fig. 3 illustrates the effect of dielectric saturation by comparing the susceptibility α and the effective susceptibilities $\alpha_{eff}(q = 1/4)$ and $\alpha_{eff}(q = 1)$. Saturation is clearly not important when finite charges of 1 au and ¼ au are considered. The differences between the three test charges are estimated to be within the statistical error of the calculation.

Fig. 4 illustrates the convergence of the susceptibility as a function of the length of the simulation. The 60-ps trajectory segment is compared with a separate 30-ps segment, and to a 15-ps segment. (The 15-ps result is actually an average of the results given by two separate 15-ps segments, the two halves of the 30-ps segment.) Because of computational cost, exact calculations were not done on longer trajectory segments. However, the approximate, analytical, small-fluctuation expression of α can easily be used with very long time-segments.

Fig. 5 compares the analytical calculation to the "exact" calculation; three analytical calculations are shown, corresponding to time-segments of 60, 120, and 150 ps, respectively. The agreement is good, with an absolute r.m.s. difference between the exact calculation and the 150-ps analytical calculation of only 0.13 Å^3. The largest deviation is at the helix C-terminus, where the displacements are large, and the analytical approximation not as good. The analytical results show a systematic increase with the length of the trajectory. The difference between 120 and 150 ps is small, indicating that the Boltzmann averaging has essentially converged after 150 ps.

To assess the correlation between the susceptibility and the local atomic mobility somewhat, we decomposed the susceptibility into two parts. The first part does not include the correlations between different atoms; rather it is obtained from the sole diagonal elements of the correlation matrix **M**. It is a sum of terms of the form

$$\frac{q_i^2\langle u_i^2\rangle_0}{r_{iq}^4}.$$

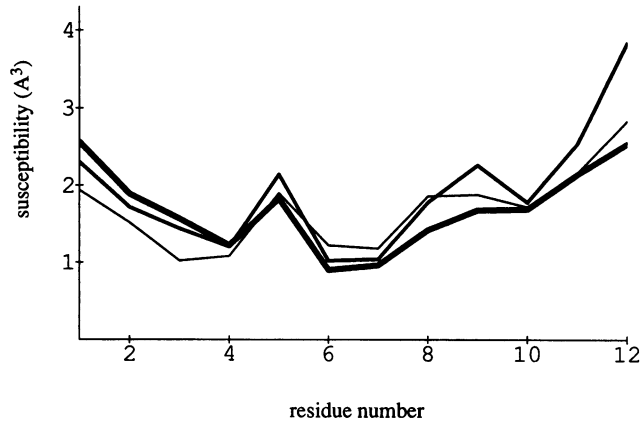

FIGURE 3 Effective susceptibilities $\alpha_{eff}(q)$ (Å^3) of deca-alanine, for different finite charges, as a function of residue number. Vanishingly small charge (*bold*), ¼ au charge (*medium*), and 1 au charge (*light*).

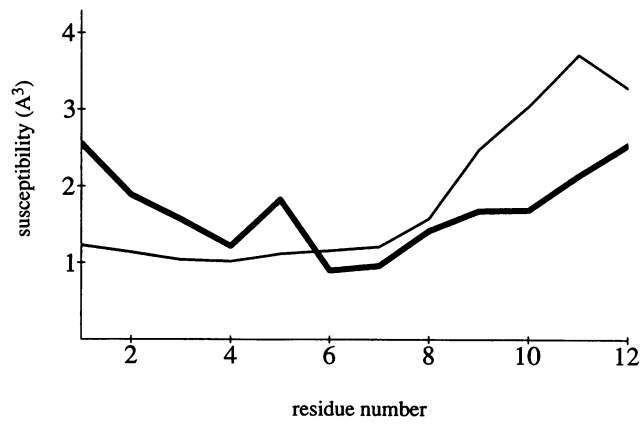

FIGURE 2 Susceptibility α(Å^3) of deca-alanine as a function of residue number. Molecular dynamics (*bold*); normal modes (*light*).

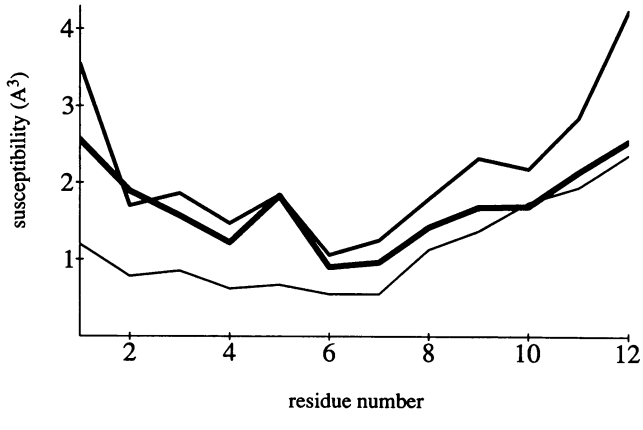

FIGURE 4 Susceptibilities (Å^3) of deca-alanine, for different trajectory lengths, as a function of residue number. 60 ps (*bold*), 30 ps (*medium*), and 15 ps (*light*).

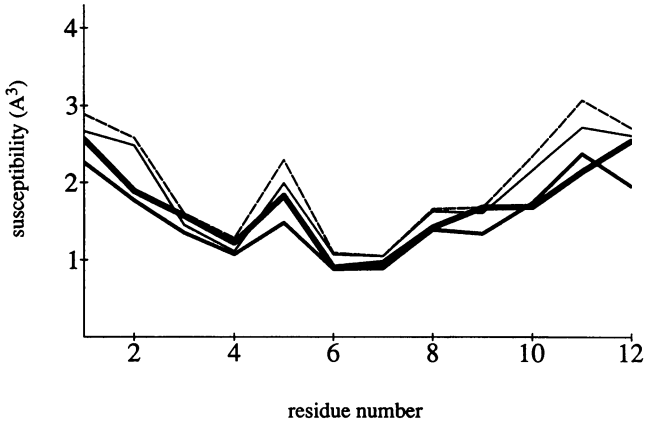

FIGURE 5 Comparison of exact susceptibility (Å³) of deca-alanine, using 60 ps trajectory (*bold*), to the small-fluctuation limit, using 150 ps trajectory (*light dashed*), 120 ps trajectory (*light*), and 60 ps trajectory (*medium*).

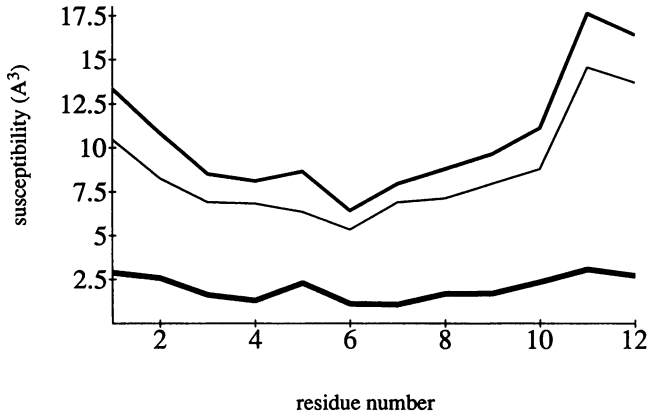

FIGURE 6 Diagonal, off-diagonal, and total contributions to the susceptibility of deca-alanine, calculated from the complete 150 ps trajectory. The off-diagonal term is multiplied by −1 for clarity. Total susceptibility (*bold*), diagonal contribution (*medium*), and off-diagonal contribution (*light*).

It is thus a weighted sum involving the local mobility, the local polarity, and the proximity of the test charge. The second part is the remaining, "off-diagonal," part of the susceptibility. The second term is more complex, and involves the cross-correlations between atoms. The diagonal contribution represents, roughly, the interaction of the test charge with the polarization it induces; the off-diagonal contribution represents the interaction of this polarization and itself. The correlation coefficient between the complete susceptibility and its diagonal part may be taken as a useful measure of the relationship between the susceptibility and the local mobility and polarity. This correlation coefficient is found in this case to be 0.68. Fig. 6 shows the decomposition of the (analytical) susceptibility obtained from the 150-ps trajectory into its diagonal and off-diagonal parts. The total susceptibility appears as a small difference between two large quantities. The details of this small difference are a function of the correlations between atomic fluctuations in the vicinity of the test charge, as much as of the local mobility and polarity.

4. CYTOCHROME C RESULTS

Structure and fluctuations of cytochrome c

The r.m.s. deviation of the mean simulated structure from the initial x-ray structure is 2.1 Å, including all heavy atoms. The deviation for different classes of atoms is shown in Table 5, which also includes data corresponding to three successive segments of the trajectory. The evolution of the potential energy and the temperature during the course of the simulation are shown in Figs. 7 and 8. The potential energy exhibits a slow and irregular drift, underlying the higher frequency, random fluctuations. This drift reflects the exploration of successive, and progressively lower, energy minima by the computer model, since the starting crystal structure is not a global energy minimum in vacuum conditions. The deviation of the calculated atomic positions from the observed values exhibits a similar drift. The r.m.s. atomic fluctuations have an average value of 0.65 Å. The value derived from the harmonic approximation was 0.38 Å. The molecular dynamics values are in good agreement with values derived from the experimental Debye-Waller factors (Table 6, Fig. 9). To extract the intramolecular fluctuations from the experimental Debye-Waller factors, the

TABLE 5 R.m.s. deviation from x-ray structure

	overall	30–60 *ps*	60–90 *ps*	90–120 *ps*
all atoms	2.06	2.01	2.10	2.21
heme	0.81	0.79	0.83	0.93
protein	2.10	2.06	2.15	2.26
backbone	1.66	1.61	1.70	1.78
side chains	2.34	2.30	2.39	2.51
6 Å shell	1.44	1.26	1.52	1.67
9 Å shell	1.49	1.40	1.55	1.67
12 Å shell	1.55	1.53	1.57	1.67
15 Å shell	2.45	2.36	2.46	2.63
18 Å shell	2.55	2.58	2.63	2.65

Root mean square deviation (Å) of cytochrome *c* simulation from x-ray structure. Results are given for several classes of atoms, and for atoms within different spherical shells. The 6-Å shell designates atoms <6 Å from the molecular centroid. The 9-Å shell designates atoms between 6 and 9 Å from the centroid; and so on.

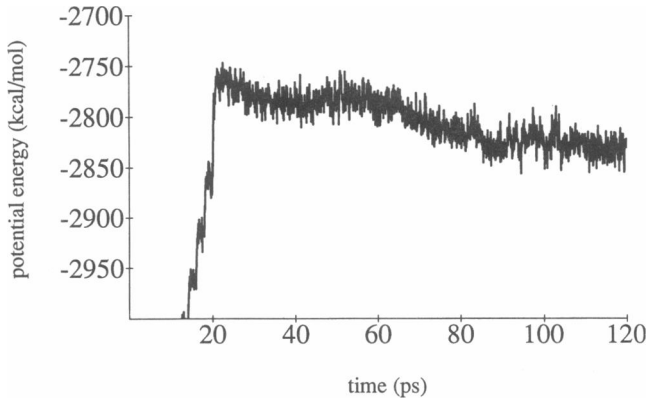

FIGURE 7 Potential energy (kcal/mol) of cytochrome *c* simulation as a function of time.

latter were uniformly corrected for translational disorder by Northrup et al. (42), using an *ad hoc* procedure involving one adjustable parameter. This procedure required that the average values of the corrected temperature factors for the interior atoms be equal to the simulated values. The corrected values were taken directly from the paper of Northrup et al., and have not been readjusted to fit our results.

Fröhlich-Kirkwood dielectric constant of cytochrome c

As in the case of deca-alanine, we calculated the Fröhlich-Kirkwood dielectric constant of cytochrome *c*, viewed as a macroscopic dielectric sphere. The value of ϵ_∞ was previously estimated to be 2.0. The overall dielectric constant in the harmonic case was estimated

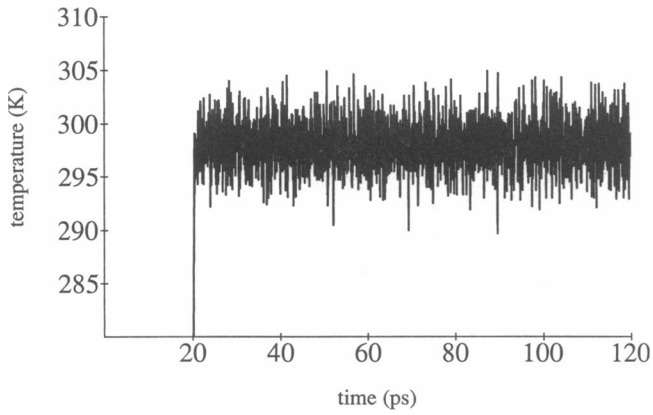

FIGURE 8 Temperature (K) of cytochrome *c* simulation as a function of time.

TABLE 6 **Simulated r.m.s. atomic fluctuations**

	X-Ray	Molecular dynamics	Harmonic
all atoms	0.66	0.65	0.38
heme	0.52	0.45	0.29
protein	0.66	0.66	0.38
backbone	0.59	0.53	0.31
side chains	0.75	0.74	0.41
6 Å shell	0.54	0.58	0.35
9 Å shell	0.56	0.55	0.34
12 Å shell	0.60	0.62	0.34
15 Å shell	0.71	0.68	0.37
18 Å shell	0.85	0.76	0.42

Simulated r.m.s. fluctuations (Å) in cytochrome *c*. Results are given for several classes of atoms, and for atoms within spherical shells of different radii. The harmonic (*light*) and x-ray (*dotted*) results are also given.

to be 2.9. In the molecular dynamics case, we obtain 3.5. The charged surface side chains are mostly responsible for this increase. If the charges of these side-chains are scaled by a factor of 0.3, as is sometimes done in molecular dynamics simulations, a dielectric constant of 2.8 is obtained. This latter result can be taken to represent the dielectric constant of the protein *interior*. In the harmonic approximation, scaling charged surface residues by 0.3 (or zero) has only a slight effect, reducing the dielectric constant to 2.5. In this approximation, the charged surface side chains are constrained to be in a local energy minimum, and cannot perform particularly large motions. These results are grouped in Table 7.

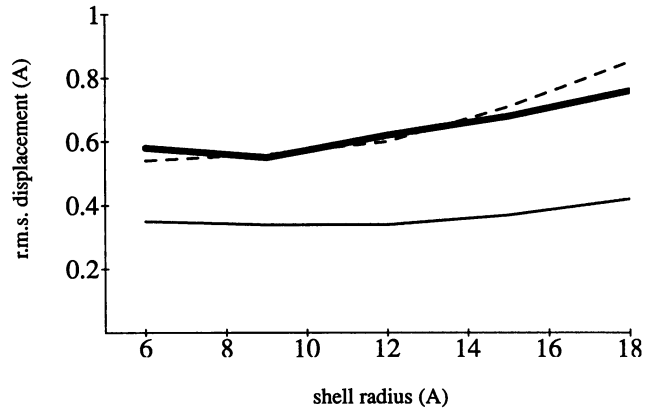

FIGURE 9 R.m.s. fluctuations (Å) in cytochrome *c* in concentric spherical shells, as a function of the shell's outer radius. For example, the 6-Å point is an average over all atoms <6 Å from the molecule's center. The 9-Å point corresponds to points between 6 and 9 Å from the center. Molecular dynamics (*bold*), x-ray (*dashed*), and harmonic (*light*).

TABLE 7 **Fröhlich-Kirkwood dielectric constant of cytochrome c**

Calculation protocol	ϵ
NM	2.9
NM, surface charges multipled by 0.3	2.5
MD	3.5
MD, surface charges multiplied by 0.3	2.8

Dielectric constant of cytochrome *c* estimated from the molecular dynamics (MD) and normal mode (NM) simulations. The molecular radius is 17 Å and $\epsilon_\infty = 2.0$.

Dielectric behavior of cytochrome c

To probe the spatial variation of the dielectric properties throughout the cytochrome *c* molecule, a perturbing test charge was placed successively on each of the 104 α-carbons of the polypeptide chain, and the corresponding susceptibility calculated. The average susceptibilities are given in Table 8, along with the variances along the polypeptide chain. (As with deca-alanine, note that these are spatial variances, unrelated to the statistical errors.) The different components of the interaction free energy of the charge with the surrounding protein are given as well. The average susceptibility was found to be $\langle\alpha\rangle = 1.57$ Å^3. This value is smaller than the value of 1.9 Å^3 previously obtained using the harmonic approximation, despite the fact that the r.m.s. atomic fluctuations are larger in the molecular dynamics calculation. The mean electronic susceptibility was previously estimated to be 0.73 Å^3. We see that for a finite charge of $q = 1$ au, the total interaction free energy A_{tot} can be as large in magnitude as -60 to -100 kcal/mol/e. The relaxation free energy A is quite large compared with the static part A_{static}. However we should note that for such large free energies, our simple, one-step, perturbation calculation is very crude; it is really meant to be used for smaller, partial charges.

TABLE 8 **Susceptibilities averaged over the α carbons of cytochrome c**

	Molecular dynamics	Normal modes
α	1.57 (0.66)	1.90 (1.12)
$\alpha_{eff}(q = 1/4)$	1.40 (0.52)	—
$\alpha_{eff}(q = 1)$	0.70 (0.20)	—
α_{elec}	0.73 (0.03)	—
A_{static}	−4.1 (24.7)	—
$\lvert A_{static}\rvert$	18.4 (16.9)	—
$A(q \to 0)$	−38.7 (15.3)	−54.4 (39.0)
$A(q = 1/4)$	−34.7 (10.5)	—
$A(q = 1)$	−17.1 (3.5)	—
A_{elec}	−23.5 (4.0)	—

Dielectric susceptibility (Å^3) of cytochrome *c* averaged over the α-carbons of the polypeptide chain. The variances over the polypeptide chain are given in parentheses. Molecular dynamics and normal mode results.

The variation of the dipolar susceptibility α along the polypeptide chain is shown in Fig. 10. This figure also shows the r.m.s. fluctuation of each residue around its mean position. The location of charged side chains is also indicated. As in the case of deca-alanine a correlation is seen between the susceptibility and the local mobility and polarity. Near the large peak at residues 85–88, for example, the mobility is very large and at the same time there is a concentration of charged residues. We can calculate the direct contribution of the charged residues to the susceptibility, to quantify further the relationship between local mobility and polarity. The resulting C_α susceptibilities have an average value of only 0.46 Å^3 and a standard deviation of 0.77 Å^3. The correlation coefficient between the complete susceptibility and the contribution of the charged residues is 0.59.

The susceptibility is also correlated with the distance of the α-carbon from the center of the molecule, or alternatively, its distance from the surface. Fig. 11 shows the susceptibility as a function of the α-carbon's distance from the molecule's centroid. These values are given as a scatter-plot. A smoothed curve is obtained by averaging the values over 1 Å spherical shells, centered at the molecule centroid. The smoothed harmonic values are also shown for comparison. The susceptibility at the iron atom of the heme group was found to be 0.63 Å^3, less than half of the average value. The dipolar susceptibility increases strongly near the protein surface. This contrasts with the electronic susceptibility, which is virtually

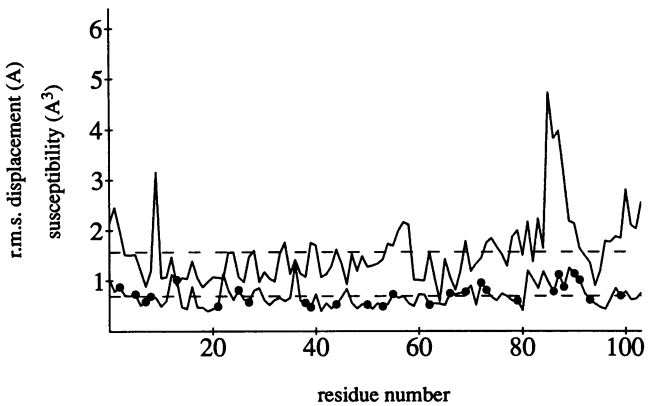

FIGURE 10 R.m.s. fluctuations (Å) of each residue (*lower curve*), and susceptibility α (Å^3) at the α-carbon (*upper curve*), as a function of the residue number. (Residue zero represents the methyl carbon blocking the *N*-terminus.) The two dashed lines indicate the average values for the two curves. Dots superimposed on the lower curve signal the location of charged residues along the polypeptide chain.

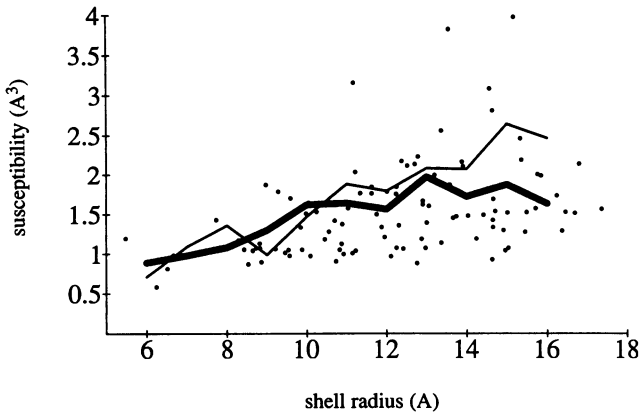

FIGURE 11 Susceptibility α (Å³) at the cytochrome *c* α-carbons as a function of their distance (in Angstroms) from the molecule's centroid. The molecular dynamics susceptibilities are shown as a scatterplot, and as a smoothed curve, where the susceptibilities are averaged over concentric spherical shells of 1 Å thickness. Smoothed curves are given for the molecular dynamics (*bold*) and harmonic (*light*) results.

uniform throughout the molecule, as shown by its small variance.

To estimate the spatial range of the dielectric screening, we calculated the susceptibility at each α carbon using an increasingly small cutoff for the electrostatic interactions. For convenience, this was done in the context of the normal mode approximation. The cutoff for the normal mode calculation was *not* varied, but only the cutoff used to derive the susceptibility from the normal modes. The results are shown in Fig. 12. The mean susceptibility decreases with increasing cutoff, converging to 1.90 Å³ for a cutoff >12 Å. With a 6-Å cutoff sphere, the mean susceptibility is 2.3 Å³, just 22% greater than the exact result. This behavior is due to the correlations between atoms within the cutoff sphere and those without. Indeed, the susceptibility decreases with the size of the cutoff sphere because the more distant atoms are not very effective in screening the test charge, but exert constraints (of an electrostatic nature) on the orientation of the inner atoms. The more distant atoms do not directly provide much additional screening, but they do limit the freedom of the inner charges to reorient themselves in response to the perturbation.

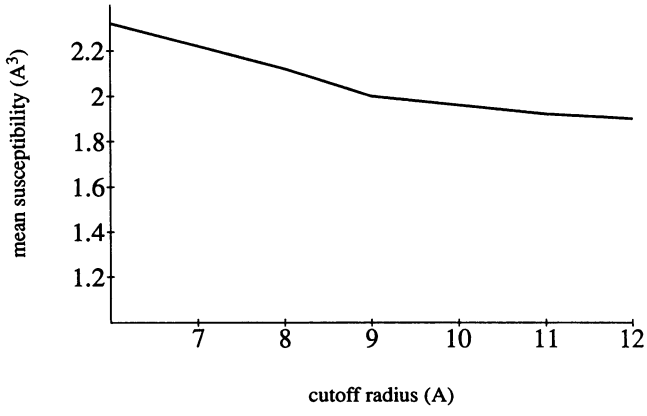

FIGURE 12 Mean susceptibility α (Å³) at the cytochrome *c* α-carbons as a function of the radius (Å) of the cutoff sphere used in the susceptibility calculation. The normal mode approximation was used. (The cutoff for the normal mode calculation is fixed at 12 Å).

As in the case of deca-alanine, dielectric saturation was investigated by considering two finite charges of 1 au and ¼ au. The average effective susceptibilities obtained with these test charges are $\alpha_{eff}(q = ¼) = 1.40$ Å³ and $\alpha_{eff}(q = ¼) = 0.70$ Å³, respectively (Table 8). The spatial variation of these susceptibilities is shown in Figs. 13 and 14. For the test charge $q = 1$ au, the effective susceptibility is attenuated by more than one half as a result of dielectric saturation, and the spatial variation of the susceptibility is greatly reduced.

To test the validity of the small-fluctuation limit, and test how well the correlation matrix **M** approaches the full susceptibility operator, we calculated the correlation matrix for that part of the structure within 8 Å of the heme. This matrix was then used to estimate the susceptibility of the heme atoms. The results were compared with the harmonic results and the exact results. The three mean values, the absolute r.m.s. deviations, and the mean correlation coefficients between the three calculations are given in Table 9. The absolute r.m.s. deviation is defined as

$$D = \left\{1/n \sum_{i=1}^{n} (\alpha_i^{(1)} - \alpha_i^{(2)})^2\right\}^{1/2}; \quad (40)$$

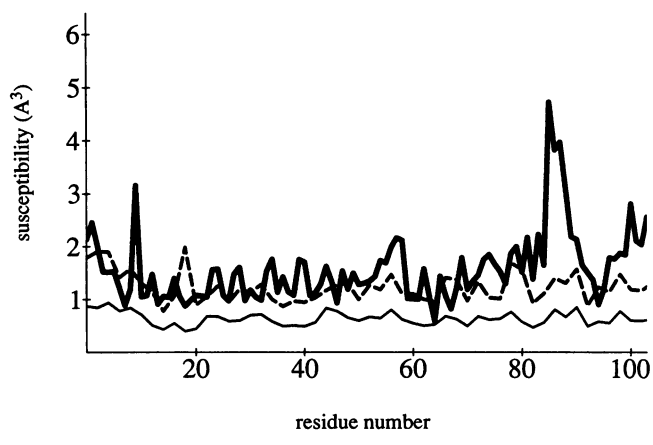

FIGURE 13 Susceptibilities α (*bold*), $\alpha_{eff}(q = ¼)$ (*medium, dashed*) and $\alpha_{eff}(q = 1)$ (*light*) (Å³) at the cytochrome *c* α-carbons as a function of residue number.

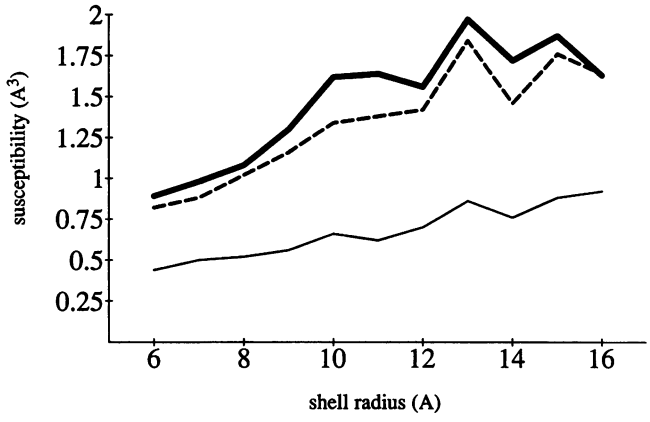

FIGURE 14 Susceptibilities α (*bold*), $\alpha_{eff}(q = 1/4)$ (*medium, dashed*), and $\alpha_{eff}(q = 1)$ (*light*) (Å³) at the cytochrome *c* α-carbons as a function of their distance from the molecule's centroid.

the sum is over the heme atoms. The mean correlation coefficient is defined as

$$C = \frac{\sum_{i=1}^{n} (\alpha_i^{(1)} - \alpha_{mean}^{(1)})(\alpha_i^{(2)} - \alpha_{mean}^{(2)})}{\left\{\sum_{i=1}^{n} (\alpha_i^{(1)} - \alpha_{mean}^{(1)})^2\right\}^{1/2} \left\{\sum_{i=1}^{n} (\alpha_i^{(2)} - \alpha_{mean}^{(2)})^2\right\}^{1/2}}; \quad (41)$$

α_{mean} denotes the average susceptibility of the heme atoms. The correlation between the exact and the small-fluctuation results is 52%; and the correlation between the small-fluctuation and harmonic results is 56%. The exact and harmonic results have only a 24% correlation over the heme. The absolute r.m.s. differences between the three calculations are fairly small, however.

Convergence of the Boltzmann averaging was examined by comparing the two halves of the trajectory. The α carbon susceptibilities as a function of residue number

TABLE 9 Correlation between three heme susceptibility calculations

		Exact	Analytical	Harmonic
	Mean (variance)	0.84 (0.12)	0.53 (0.14)	0.57 (0.19)
Correlation	Exact	100	52	24
	analytical		100	56
	harmonic			100
R.m.s. deviation	Exact	0	0.34	0.34
	analytical		0.	0.17
	harmonic			0.

Mean values (Å³), absolute r.m.s. differences (Å³), and correlation coefficients (percent) of the three susceptibility calculations on the heme atoms.

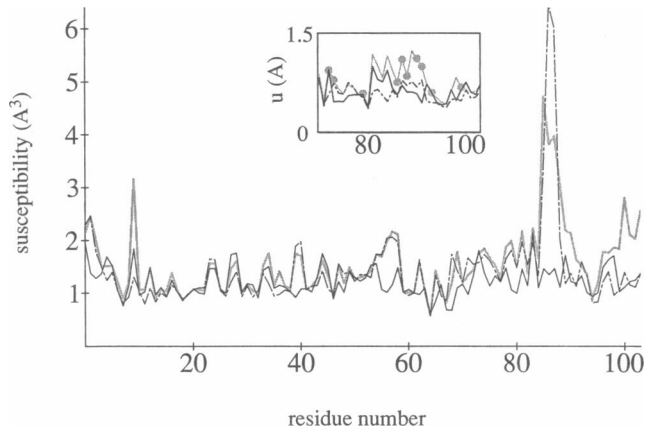

FIGURE 15 Susceptibilities on the α carbons as a function of residue number, calculated from the full 90 ps trajectory (*light*), and the two 45-ps halves of the trajectory (*dark*). (*Insert*) R.m.s. atomic displacement *u* (Å) averaged over each residue as a function of residue number, calculated from the full 90 ps trajectory (*light*), and the two 45-ps halves of the trajectory (*dark*). The grey dots signal the location of charged residues along the polypeptide chain. The dot-dash curves correspond to the first half of the trajectory.

are shown in Fig. 15 for each half of the trajectory. The peak in the 85–88 region is absent in the second half of the trajectory. At the same time, the mobility of the charged residues in this region is reduced during this half of the trajectory. Near the midpoint of the trajectory, the residues Lys 87, Lys 88, and Glu 90 all undergo conformational changes, as shown in Fig. 16. These changes appear to be responsible for the change in local dielectric properties.

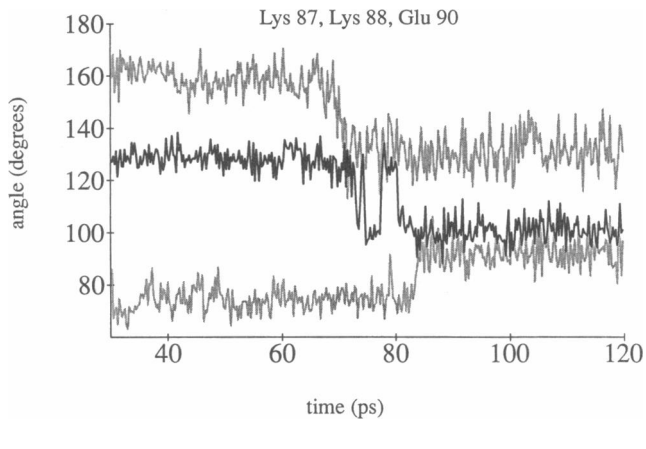

FIGURE 16 The angle N–C_α–N_ζ plotted as a function of time for lysines 87 (*light, lower*) and 88 (*light, upper*); the angle N–C_α–C_δ as a function of time for Glu 90 (*bold*).

5. DISCUSSION

The results of the preceding sections call for a number of comments. In this section we first consider the results on deca-alanine, then the results on cytochrome *c*, and finally we examine their implications for our working hypothesis: a functional variation of the susceptibility in proteins.

Analysis of the deca-alanine results

The calculated fluctuations of the helix are consistent with previous studies of deca-glycine (43, 44). The calculated r.m.s. displacements of the previous and present studies, for all but the two terminal residues and their blocking groups, are 0.39 and 0.35 Å, respectively in the harmonic case, and 0.58 and 0.45 Å with full molecular dynamics at 300 K. Thus, for deca-glycine, Levy et al. observed r.m.s. molecular dynamics fluctuations at 300 K about one and a half times as large as the harmonic fluctuations. They noted that the radial displacements, along the direction normal to the helix axis, were approximately harmonic at room temperature. We find that the whole central part of deca-alanine behaves very much as in the harmonic model, with only the first and last alanines and their blocking groups deviating strongly from this behavior. Because of this, it is not surprising that the dielectric behavior of the helix is calculated to be similar to our previous, harmonic results (1). The average dipolar susceptibility, 1.77 Å^3, is close to its harmonic value of 1.58 Å^3. This is almost double the electronic susceptibility. We can extrapolate our previous conclusion, that the electrostatic coupling between these two types of relaxation is a small corrective effect.

The free energy of interaction between the test charge and the helix is quite large near the helix termini. For a negative charge near the *N*-terminus, the total perturbation free energy can be as large as −30 kcal/mol/e, though the test charge is located 4 Å away from the helix. The contribution of dipolar relaxation, *A*, represents typically ~25% of this.

The spatial variation of the dipolar susceptibility is large, with several differences from the harmonic behavior. The susceptibility is over 2.5 Å^3 at both ends of the helix, and close to 1 Å^3 in the middle. Note that residue 5, where the susceptibility is large, is spatially adjacent to the *N* terminus. The large terminal susceptibilities are clearly correlated with the larger mobility and polarity of these regions: there are two *NH* groups not involved in hydrogen bonds at the *N* terminus, and two *CO* groups at the *C* terminus. We saw in Materials and Methods that soft fluctuations of polar groups give rise to a large susceptibility, because these groups can move extensively along their soft degrees of freedom in response to a perturbation. In this case, not only are hydrogen bond donors or acceptors present, but they are mobile, and therefore available to screen perturbing charges. In the harmonic case however, the large *N* terminal susceptibility is absent. This discrepancy is due to at least two factors. First of all, in the harmonic case, the *N* terminus is no more mobile than the helix middle; both have an r.m.s. displacement of 0.37 Å (*O* and *H* atoms). The *C* terminus has an r.m.s. displacement of 0.43 Å. Second, we saw that the susceptibilities are small differences between a positive, diagonal contribution, and a negative, off-diagonal contribution. Both contributions explicitly depend on local polarity and mobility, while their difference is largely determined by the correlations between atomic fluctuations. Thus, we expect that subtle differences in local dynamics can produce fairly large differences in susceptibilities. Indeed, the correlation coefficient between the complete susceptibility and its diagonal part is only 0.68. It is interesting to note that the overall shape of the harmonic susceptibility curve is quite similar to that of the 15 ps molecular dynamics results (Fig. 4). This suggests that anharmonic effects become significant in this system on a time-scale longer than 15 ps.

In the harmonic case, a few low-frequency modes of vibration account for the spatial variation of the susceptibility (1). With full molecular dynamics, a quasiharmonic analysis of the trajectory would be needed to investigate this possibility. However, the nearly harmonic behavior of the helix, and the rough agreement of the susceptibilities, suggest that the same conclusion may carry over to the anharmonic case.

The Boltzmann averages have not converged after 60 ps of simulation; the small-fluctuation results show that ~150 ps are necessary for convergence. This is especially true near the helix termini, where the mobility is greater, and more conformations are available to the structure. Given the smooth, systematic difference between the analytical results for different time-segments, it seems unlikely that further averaging will change any of our results qualitatively. The small-fluctuation results agree quite well with the exact ones when residue averages are compared, as in Fig. 5. The largest difference is at the *C* terminus, where the large atomic displacements affect the accuracy of the analytical calculation. The first term neglected in the small-fluctuation susceptibility is on the order of $(u_i/r_{iq})^4$, where *i* is a helix atom. For our 4-Å surface, and near the *C* terminus, $u_i/r_{iq} \approx 1/4$, and $(u_i/r_{iq})^4 \approx 1/256$. Since the observed difference between exact and small-fluctuation results is much larger than 0.4%, higher order terms must be contributing to the exact results. The exact susceptibility tends to be larger than the small-fluctuation result, suggesting

that the exact result would eventually converge to values somewhat larger than the 150 ps small-fluctuation values.

Dielectric saturation was estimated by considering finite test charges of 1 and ¼ au. The relaxation free energies for these charges were calculated in a single perturbation step (Eq. 9). This is known to be inaccurate for energies much greater than kT (e.g., reference 45). For our ¼ au charge, the relaxation free energies are about −0.2 kcal/mol on average (Table 4). Therefore our estimate of dielectric saturation is expected to be quite accurate for this charge. For the 1-au charge, the relaxation energies are about −3 kcal/mol on average. For such large energies, the trajectory of the unperturbed helix does not sample enough of the conformations where $exp(-\beta V)$ is large, V being the interaction energy between the perturbing charge and the helix. These are the conformations made probable by the perturbing charge. Because of this the quantity $exp(-\beta A)$ is underestimated, the relaxation free energy A is overestimated, and the effect of saturation is *overestimated.* This sampling error can be viewed as an underestimate of the effect of electrostriction (as defined by Jayaram et al. [47] in their analysis of dielectric saturation around ions in water). For the 1-au charge, our estimate of saturation is therefore rough, though probably of the right order of magnitude. We see that the dielectric saturation is not significant when the ¼ au and 1 au charges are considered. The field of the 1 au test charge at the nearest deca-alanine atoms is $\sim 10\ kT/e/$Å. Alper and Levy (46) found that in molecular dynamics simulations of water, the polarization response to an external field E was linear in the range $E < 0.1\ kT/e/$Å and nonlinear beyond. Jayaram et al. (47) analyzed the polarization of water surrounding an ion in Monte Carlo simulations, and observed a linear response up to at least 10–20 $kT/e/$Å. Note that saturation is expected to occur for lower fields in proteins than in water, because they are much less polarizable than water.

One final comment concerns the agreement between the microscopic dielectric model and the macroscopic continuum model. These two models are compared in Fig. 17. The electronic susceptibility α_{elec} is compared with the susceptibility calculated from a finite-difference continuum model, using a dielectric constant of 1.7 for the helix (the estimated high-frequency dielectric constant of deca-alanine). The results are taken from reference 1. The total susceptibility $\alpha + \alpha_{elec}$ is also compared with a continuum calculation, using a dielectric constant of 3 for the helix. This value was chosen to optimize approximately the fit between the macroscopic and microscopic calculations. The total susceptibilities calculated using the continuum model do not agree with the microscopic susceptibilities $\alpha + \alpha_{elec}$ calculated here,

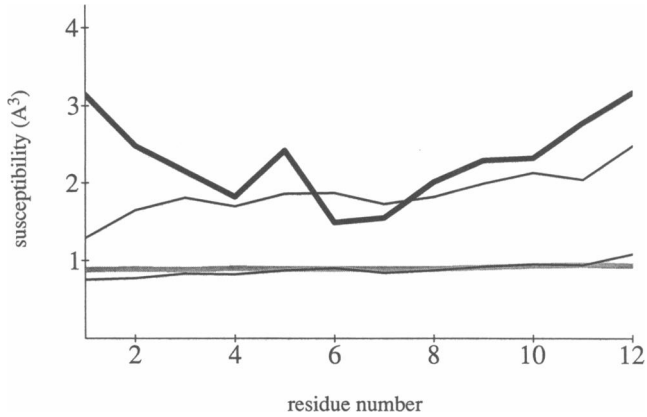

FIGURE 17 Comparison between the susceptibilities of deca-alanine calculated from our microscopic approach and those calculated from a continuum model. (*Lower two curves*) Electronic susceptibility as a function of residue number (*solid*); continuum calculation (*dashed*) using the high-frequency dielectric constant, 1.7, of deca-alanine. (*Upper two curves*) Total susceptibility (electronic + dipolar) as a function of residue number (*solid*); continuum calculation (*dashed*) using a dielectric constant of 3 (chosen to approximately optimize the fit between the two).

any more than they agreed with our previous, harmonic results. Their average value (1.29 Å³) could be adjusted further; but their spatial variability (standard deviation 0.25 Å³) is markedly too small. In contrast, the continuum model does reproduce the nearly uniform electronic susceptibilities very well.

Analysis of the cytochrome c results

Tuna ferricytochrome *c* contains four aspartates, five glutamates, two arginines, and sixteen lysines. The heme charge is −2 au, and the terminal groups were modeled as neutral, so the overall charge is +7 au, and the molecule has a strong positive overall potential. The *in vacuo* simulation obviously does not account for screening of this potential by solvent molecules or counterions. This will have a large effect on the calculated susceptibilities.

The behavior of the simulation is consistent with previous simulations of cytochrome *c in vacuo* (42), with a similar deviation from the x-ray structure (2.1 Å) and similar r.m.s. fluctuations for different groups of atoms. The r.m.s. fluctuations also agree closely with those derived from experimental Debye-Waller factors. Actually, recent work has shown that the Debye-Waller factors from refined protein structures effectively contain little information about the internal dynamics of proteins, but reflect mainly the overall translation libration of the molecule (48). What information there is agrees with our results. The mobility is greater than in

the harmonic calculation, and increases more sharply near the molecule's surface. The r.m.s. fluctuation of the charged surface side chains, for example, is 0.91 Å, compared with 0.74 Å for all side chains. In the harmonic case, charged and uncharged side chains both have an r.m.s. fluctuation of 0.41 Å. At the molecule's surface the molecular dynamics fluctuations are thus double the harmonic ones.

The free energy of interaction of the test charge with the protein is large, and the component due to dielectric relaxation is also large. The magnitude of the static term ($|A_{static}| \sim 18$ kcal/mol/e) is consistent with values of protein charge–charge interactions in bovine pancreatic trypsin inhibitor (49). The electronic contribution A_{elec} to A_{tot} is -23 ± 4 kcal/mol/e, which is larger than the values calculated by Russell and Warshel (49) for ionizing various side chains in BPTI; their average electronic contribution for four side chains is only -4.2 kcal/mol/e. However, since their calculation included the surrounding water, it is possible that the electronic relaxation within the protein was affected by the solvent relaxation.

The calculated dielectric behavior of cytochrome *c* is consistent overall with that of deca-alanine, of several other helical polypeptides (1), as well as of the disk of protein of tobacco mosaic virus (Simonson and Perahia, unpublished results). It is also much more complex than that of deca-alanine, due to the numerous charged groups, the larger anharmonicity, the increased possibility of local conformation changes, and the difficulty in calculating accurately mean fluctuations, given the large number of degrees of freedom. These difficulties are aggravated because the charged groups are unscreened by solvent, and the calculations are therefore very sensitive to the details of their dynamics. One consequence of this is that the agreement of the molecular dynamics susceptibilities with the harmonic susceptibilities is poor. The mean values for the α carbons are similar: 1.77 Å^3 and 1.90 Å^3, respectively. However, the absolute r.m.s. difference between the two sets is 1.35 Å^3. Despite the greater molecular dynamics fluctuations, the susceptibilities calculated by molecular dynamics are slightly smaller than the harmonic results, with a particularly large discrepancy at the protein surface (Fig. 11). This is evidently the opposite trend to what we would expect from the local mobility. This discrepancy is due to at least three factors. The first factor is the uncertainty of the susceptibilities of the surface regions, due to the uncertainty of the Boltzmann sampling, especially in the absence of solvent screening. The second factor is the importance of interatomic correlations in determining the susceptibility. We saw in the case of deca-alanine that these correlations are just as important as the local mobility/polarity, because of cancellations between the diagonal and off-diagonal parts of the susceptibility operator. The third factor is that the harmonic susceptibilities, unlike the molecular dynamics susceptibilities, were calculated in the small-fluctuation limit.

Nevertheless, the conclusions of our previous study remain valid, for the molecular dynamics results exhibit the same qualitative features as the harmonic ones. The mean value is similar, and is again more than double the mean electronic susceptibility of 0.73 Å^3. The spatial variation along the polypeptide chain is smaller than in the harmonic case, but still quite large. Most importantly, the susceptibility, when averaged over spherical shells, is again found to increase regularly going from the center of the molecule to its surface. The susceptibilities on the heme atoms are again particularly weak. The susceptibility on the iron atom is, for example, 0.63 Å^3, less than half the average value. The average susceptibility on the heme is 0.83 Å^3.

There are five regions along the polypeptide chain where the susceptibility is above average: at Thr 9, at residues 54–58, around the large 85–88 peak, and at the two termini. The susceptibility at a given α carbon is a local property, determined by short-range charge-dipole interactions. Indeed, except for the 54–58 region, the susceptibility peaks are all in regions where the local mobility is greater than average, particularly the 85–88 region. The concentration of charged side chains is quite large in two of these regions, the *N*-terminus and the 85–88 region. More generally, the increase of the susceptibility near the protein surface is correlated with increasing mobility and polarity. At the same time though, the direct contribution of the charged residues to the susceptibility only represents 0.46 Å^3 on average, and has a correlation with the full susceptibility of just 59%. Thus it is not altogether surprising that there is a large spread of susceptibilities for some values of the depth within the protein. As noted above, the relationship between local mobility/polarity and susceptibility appears to be fairly complex. Local correlations between the atomic displacements play an important role, with diagonal and off-diagonal parts of the dipole–dipole correlation matrix tending to cancel each other.

The importance of dielectric saturation is found to be greater than in deca-alanine. The relaxation free energies are larger in this case, so the estimate is much rougher. For a unit charge, dielectric saturation reduces the average relaxation by one half. For the ¼ au charge, although the average effect of saturation is smaller, the local effect is very large in regions of high susceptibility. For example, the peak at residues 85–88 is completely destroyed by saturation. Note that saturation effectively extends the range of dielectric screening somewhat. Indeed, when a finite perturbing charge is considered, the screening of nearby atoms is reduced by dielectric saturation. For more distant atoms, the perturbing field

is smaller and thus saturation is smaller. The relative importance of the distant atoms is therefore increased.

The validity of the small-fluctuation approximation, and thus the accuracy with which the correlation matrix **M** approaches the susceptibility operator, was examined for the heme atoms. The agreement with the exact calculation is only qualitative, with a correlation coefficient of 52% and an absolute r.m.s. shift of 0.34 Å^3 (Table 9). Since the test charges considered here are actually within the protein, the ratios u_i/r_{iq} are larger than in the deca-alanine case, i.e., the fluctuations are effectively larger. The analytical calculation does reproduce the most important feature of the exact calculation, the low overall heme susceptibility.

The convergence of the Boltzmann averaging as a function of trajectory length is illustrated in Fig. 15. This figure shows the susceptibility at each α carbon as a function of residue number, for three time segments: the full 90-ps time segment, and its two 45-ps halves. There are large susceptibility differences between the two halves of the trajectory in certain parts of the chain. In particular, the largest susceptibility peak, around residues 85–89, is completely absent when only the second half of the trajectory is considered (t = 75 to t = 120 ps). When the r.m.s. fluctuations are calculated from the second half of the trajectory, the mobility of this region is also changed. The charged residues Lys 86–88, Glu 90, and Arg 91 all have significantly reduced mobilities. Fig. 16 suggests that this is due to conformational shifts that occur during the simulation. The charged residues Lys 87, Lys 88, and Glu 90 all undergo sharp reorientations near the midpoint of the data collection. In other words, a local, probably concerted, conformation change occurs involving a few charged residues, modifying the local structure and dynamics, and completely modifying the local dielectric properties. This shows that it is difficult to sample all the relevant conformation states during a short simulation, and difficult to establish convergence of the sampling. This also shows that different conformational substates can exist with different local dielectric properties. This may have biological significance, since in charge-transfer proteins, for example, catalytic activity depends directly on local dielectric properties. In addition, this kind of conformational substate could perhaps be observed experimentally by spectroscopic measurements, such as fluorescence measurements. Indeed, in some proteins, the lifetime of the fluorescent excited state is mainly determined by the charge transfer properties of the fluorophore environment. The rate of decline of the fluorescence anisotropy would then be affected by changes in the local dielectric properties produced by conformational changes. If discrete substates exist, as in our simulation, they will give rise to a discrete set of relaxation times, such as was observed recently in thioredoxin (50).

In summary, we encounter at least four difficulties when calculating the dielectric susceptibilities of cytochrome *c*. First, the susceptibility has a subtle and sensitive dependence on the local structure, dynamics, and polarity; the details of the dielectric behavior appear to be determined by the correlations between atomic fluctuations. Second, the protein contains twenty-eight charged residues and a charged heme. Free energy calculations in charged systems are intrinsically difficult (e.g., references 45 and 6). In our calculation the solvent is absent, so that these charges are largely unscreened: their charges, and the details of their fluctuations, are seen in full by much of the molecule. Third, the small-fluctuation limit (and *a fortiori* the harmonic approximation) appears to be a rough approximation when considering perturbing charges *within* the protein. Fourth, the large fluctuations make it difficult to sample completely the relevant conformation space in a short simulation. This is especially true for the important charged surface side chains. These side chains can undergo conformation changes that modify the local structure and dynamics.

Despite these difficulties, all our calculations agree as to the magnitude of the susceptibility and its overall spatial variation throughout the protein. When a spatial region such as the heme is considered in detail, the two small-fluctuation calculations (harmonic and anharmonic) are in fair quantitative agreement, and the two full molecular dynamics calculations (exact and small-fluctuation limit) agree more qualitatively. More analysis of the relationship between susceptibility, structure, and dynamics is necessary, and currently underway.

Spatial variation of the dielectric properties and its possible functional significance

We emphasized in the Introduction that in enzyme-catalyzed charge transfer reactions, the dominant contribution to the reorganization free energy comes from the solvent, due to its large dielectric constant. Nevertheless, the contribution of the protein relaxation, considered in this paper, is not negligible. In cytochrome *c* for example, the contribution of dipolar relaxation (A) to the total interaction (A_{tot}) between our test charge and the protein is estimated to be around −20 kcal/mol/e, for a finite 1-au charge. This can be compared with the interaction between a small charge in a protein and the surrounding solution, calculated roughly from a continuum model (16), and which is on the order of a few tens of kcal/mol/e. It can also be compared with the total change in solvation free energy upon ionizing an acidic

group in a protein, which is on the order of −70 kcal/mol/e (49). Clearly, although the solvent polarization may dominate enzyme reorganization free energies, there is a considerable advantage to lowering the contribution of the protein relaxation. As a result, Simonson et al. (1) suggested that enzymes may improve their efficiency by providing a dielectric susceptibility in the vicinity of the active site that is lower than in the rest of the molecule. More generally, we suggested that the spatial variation of the dielectric properties throughout a protein may have functional significance. Our results, obtained in the framework of a full molecular dynamics model, confirm and broaden the conclusions of our previous, harmonic analysis with regard to this hypothesis. First of all, they give an explicit microscopic estimate of the average importance of dielectric relaxation, including saturation effects. The susceptibilities obtained are compatible with macroscopic dielectric constants of ~2–4, as shown by the calculated Fröhlich-Kirkwood dielectric constants. Second, they give an estimate of the spatial variability of the dielectric properties in proteins, which is found to be quite large. In cytochrome *c* we observe variations of the susceptibility by a factor of three over just a few Ångstroms. These variations result from the dipolar component of the susceptibility, the electronic susceptibility being uniform. The atomic point polarizability model, in combination with a near-uniform set of polarizabilities, is evidently too simple to account realistically for inhomogeneous electronic effects, such as must arise in conjugated groups. Dielectric saturation is seen to reduce the amplitude of the relaxation in cytochrome *c*, particularly in local regions of large susceptibility.

In the two systems analyzed, deca-alanine and cytochrome *c*, the spatial variations of the susceptibility do indeed correlate with functional activity. The large susceptibilities of the deca-alanine termini are mainly due to the free hydrogen bond donor and acceptor groups. Their large fluctuations in the unperturbed helix indicate that these groups have considerable liberty to reorient themselves in response to a perturbing charge. This sheds a new light on a well-known property of α helices, their capacity to stabilize charged or polar groups in proteins. Hol [51] pointed out for example that in over twenty phosphate-binding proteins, α helices participate in the ligand-binding through hydrogen bonds at their *N* terminus. This has long been recognized as an effect of the polarity of the helix [52]. However the capacity of these terminal groups to *rearrange* themselves so as to optimize the hydrogen bonding is also a factor. The dipolar susceptibility measures precisely the importance of structural relaxation of the helix, including the terminal groups, and our results give a quantitative estimate of its magnitude. At typical ligand binding distances from the helix, the dipolar relaxation free energy of the helix is about −3 kcal/mol for a perturbing charge of 1 au. This is not a negligible contribution, notwithstanding the further contributions of the solvent, the electronic degrees of freedom, and the permanent charges of the protein. In summary, the spatial variation of the susceptibility of decalanine is compatible with, and suggestive of, a functional role for the spatial variation of the susceptibility in real α helices.

In cytochrome *c*, the importance of the dielectric properties of the protein and solvent is even clearer. These properties determine the reorganization free energy for electron transfer to and from the protein. To be precise, the susceptibility tensor of the heme atoms determines this energy. Since the protein has a low average dielectric constant, the relaxation free energy in response to charge transfer is low. What we have shown is that in the heme region of the structure, the protein's contribution to the local susceptibility is much lower than in the rest of the structure. Loosely speaking, the heme region has a local dielectric constant that is less than half the average dielectric constant of the molecule. This effect is of course small compared with the contribution of the solvent relaxation to the reorganization free energy. But it is not negligible. It must be taken into account in any quantitative analysis of electron-transfer kinetics to and from cytochrome *c*. In summary, the spatial variation of the susceptibility within cytochrome *c* is compatible with, and suggestive of, a functional role for the spatial variation of the susceptibility.

6. CONCLUSIONS

This article pursues the development of a microscopic theory of the dielectric properties of proteins. The theory combines elements of linear response theory with techniques of free energy calculation. It incorporates all the relevant contributions to dielectric screening in these systems: dipolar relaxation, electronic relaxation, and electrostatic coupling between the two. The latter two contributions were analyzed previously, while this study concentrated on dipolar relaxation. In the small-fluctuation limit simple analytical formulae are obtained.

The theory was previously presented in the context of the normal mode approximation, considering only the protein's response to perturbing point charges. We have now extended the theory to include a full anharmonic description of the system's dynamics, and to deal with the relaxation in response to an arbitrary perturbing charge density. This enables us in principle to investigate the full complexity of a protein's microscopic dielectric behavior. Several aspects have been addressed thus far,

such as the nature of the motions contributing to the susceptibility, the role of short- and long-period fluctuations, and the dependence of the susceptibility on the simulation time; the importance of dielectric saturation; how well the dipole–dipole correlation matrix represents the full susceptibility operator. The existence of two conformational substates with very different local dielectric properties was observed in the cytochrome *c* simulation. Such substates could perhaps be detected experimentally by fluorescence measurements on real proteins. We have also shown how the reorganization free energy associated with charge transfer can be calculated in this approach, in the small-fluctuation limit. Some of the difficulties and limitations of the method have been discussed. More detailed analysis of these is underway. In particular it is crucial to investigate the contribution of the solvent to the relaxation free energies.

We have applied this approach to deca-alanine and cytochrome *c* in an effort to test our working hypothesis: does the spatial variation of the dielectric susceptibility within proteins contribute to their activity? Our results suggest that the binding of charged ligands by α helices in proteins is affected not only by the presence of hydrogen bond donors at the *N* terminus, but also by the flexibility of these donors, which manifests itself in the form of a large, local, dipolar susceptibility. In the case of cytochrome *c*, the particularly low susceptibility found in the heme region implies a particularly low contribution of dipolar relaxation to the reorganization free energy for electron transfer. This in turn contributes directly to the protein's efficiency. Thus our results, although they do not constitute a proof, are indeed compatible with our working hypothesis.

A referee pointed out a missing factor ½ in the relaxation free energy. Arieh Warshel made helpful comments on the manuscript.

Received for publication 15 August 1990 and in final form 26 October 1990.

REFERENCES

1. Simonson, T., D. Perahia, and G. Bricogne. 1990. Intramolecular dielectric screening in proteins. *J. Mol. Biol.* In press.
2. Warshel, A., and M. Levitt. 1976. Theoretical studies of enzymic reactions: dielectric, electrostatic and steric stabilization of the carbonium ion in the reaction of lysozyme. *J. Mol. Biol.* 103:227–249.
3. Churg, A., R. Weiss, A. Warshel, and T. Takano. 1983. On the action of cytochrome *c*: correlating geometry changes upon oxidation with activation energies of electron transfer. *J. Phys. Chem.* 87:1683–1694.
4. Warshel, A., and F. Sussman. 1986. Toward computer-aided site-directed mutagenesis of enzymes. *Proc. Natl. Acad. Sci. USA.* 83:3806–10.
5. Hwang, J. K., and A. Warshel. 1987. Semiquantitative calculations of catalytic free energies in genetically modified enzymes. *Biochemistry.* 26:2669–73.
6. Warshel, A., F. Sussman, and J.-K. Hwang. 1988. Evaluation of catalytic free energies in genetically modified proteins. *J. Mol. Biol.* 201:139–159.
7. Warshel, A., G. Naray-Szabo, F. Sussman, and J. K. Hwang. 1990. How do serine proteases really work? *Biochemistry.* 28:3629–37.
8. Rao, S., U. Chandra Singh, P. Bash, and P. Kollman. 1987. Free energy perturbation calculations on binding and catalysis after mutating Asn 155 in subtilisin. *Nature (Lond.).* 328:551–554.
9. Krishtalik, L. 1985. Effective energy of enzymatic and non-enzymatic reactions. Evolution-imposed requirements to enzyme structure. *J. Theor. Biol.* 112:251–264.
10. Warshel, A. 1978. Energetics of enzyme catalysis. *Proc. Natl. Acad. Sci. USA.* 75:5250–5254.
11. Warshel, A. 1981 Electrostatic basis of structure-function correlation in proteins. *Acc. Chem. Res.* 14:284–290.
12. Warshel, A. 1987. What about protein polarity? *Nature (Lond.).* 330:15–16.
13. Landau, L., and E. Lifschitz. 1980. Electrodynamics of Continuous Media. Pergamon Press, New York.
14. Tanford, C., and J. Kirkwood. 1957. Theory of protein titration curves. General equations for impenetrable spheres. *J. Am. Chem. Soc.* 79:5333–5339.
15. Warwicker, J., and H. Watson. 1982. Calculation of the electrostatic potential in the active site cleft due to α helix dipoles. *J. Mol. Biol.* 157:671–679.
16. Warshel, A., S. Russell, and A. Churg, 1984. Macroscopic models for studies of electrostatic interactions in proteins: limitations and applicability. *Proc. Natl. Acad. Sci. USA.* 81:4785–4789.
17. Klapper, I., R. Hagstrom, R. Fine, K. Sharp, and B. Honig. 1986. Focusing of electric fields in the active site of Cu-Zn superoxide dismutase. *Proteins.* 1:47–59.
18. Delepierre, M., C. Dobson, M. Karplus, F. Poulsen, D. States, and R. Wedin. 1987. Electrostatic effects and hydrogen exchange behavior in proteins. The pH dependence of exchange rates in lysozyme. *J. Mol. Biol.* 197:111–130.
19. Bailey, S. 1951. The dielectric properties of various solid crystalline proteins, amino acids and peptides. *Trans. Far. Soc.* 47:509–517.
20. Rosen, D. 1963. Dielectric properties of protein powders with adsorbed water. *Trans. Far. Soc.* 59:2178–2191.
21. Takashima, S., and H. Schwan. 1965. Dielectric dispersion of crystalline powders of amino acids, peptides, and proteins. *J. Phys. Chem.* 69:4176–4182.
22. Bone, S., and R. Pethig. 1982. Dielectric studies of the binding of water to lysozyme. *J. Mol. Biol.* 157:571–575.
23. Pethig. 1979. Dielectric and Electronic Properties of Biological Materials. Wiley, New York
24. Gilson, M., and B. Honig. 1985. The dielectric constant of a folded protein. *Biopolymers.* 25:2097–2119.
25. Nakamura, H., T. Sakamoto, and A. Wada. 1988. A theoretical study of the dielectric constant of a protein. *Prot. Eng.* 2:177–183.
26. Onsager, L. 1936. Electric moments of molecules in liquids. *J. Am. Chem. Soc.* 58:1486–1493.

27. Landau, L., and E. Lifschitz. 1980. Statistical Mechanics. Pergamon Press, New York.
28. Callen, H., and Welton. 1951. Irreversibility and generalized noise. *Phys. Rev.* 83:34–40.
29. Kirkwood, J. 1939. The dielectric polarization of polar liquids. *J. Chem. Phys.* 7:911–919.
30. Fröhlich, H. 1949. Theory of Dielectrics. Clarendon Press, Oxford.
31. Stell, G., G. Patey, and Høye. 1981. Dielectric constants of fluid models: statistical mechanical theory and its quantitative implementation. *Adv. Chem. Phys.* 48:183–328.
32. Chandler, D. 1978. Structures of molecular liquids. *Annu. Rev. Phys. Chem.* 29:441–471.
33. Chandler, D. 1977. The dielectric constant and related equilibrium properties of molecular fluids: interaction site cluster theory analysis. *J. Chem. Phys.* 67:1113–1124.
34. Roux, B., H.-A. Yu., and M. Karplus. 1990. Molecular basis for the Born model of ion solvation. *J. Phys. Chem.* 94:4683–4688.
35. Karplus, M., and J. Kushick. 1981. Method for estimating the configurational entropy of macromolecules. *Macromolecules.* 14:325–332.
36. Brünger, A. 1987. *Xplor* Version 2.1, User Manual. Yale University, New Haven.
37. Brooks, B., R. Bruccoleri, B. Olafson, D. States, S. Swaminathan, and M. Karplus. 1983. CHARMM: a program for macromolecular energy, minimization, and molecular dynamics calculations. *J. Comp. Chem.* 4:187–217.
38. Ryckaert, J. P., G. Ciccotti, and H. Berendsen. 1977. Numerical integration of the Cartesian equations of motion of a system with constraints: molecular dynamics of n-alkanes. *J. Comp. Phys.* 23:327.
39. Berendsen, H., J. Postma, W. van Gunsteren, A. DiNola, and J. Haak. 1984. Molecular dynamics with coupling to an external bath. *J. Chem. Phys.* 81:3684–3690.
40. Takano, T., and R. Dickerson. 1980. Redox conformation changes in refined tuna cytochrome *c*. *Proc. Natl. Acad. Sci. USA.* 77:6371–6375.
41. Connolly, M. 1983. Analytical molecular surface calculation. *J. Appl. Cryst.* 16:548–558.
42. Northrup, S., M. Pear, J. Morgan, J. A. McCammon, and M. Karplus. 1981. Molecular dynamics of ferrocytochrome *c*. Magnitude and anisotropy of atomic displacements. *J. Mol. Biol.* 166:1087–1109.
43. Levy, R., D. Perahia, and M. Karplus. 1982. Molecular dynamics of an α helical polypeptide: temperature dependence and deviation from harmonic behavior. *Proc. Natl. Acad. Sci. USA.* 79:1346–1350.
44. Perahia, D., R. Levy, and M. Karplus. 1990. Motions of an α helical polypeptide: comparison of molecular and harmonic dynamics. *Biopolymers.* 29:645–677.
45. Straatsma, T. 1987. Free energy evaluation by molecular dynamics simulations. Ph.D. thesis. University of Groningen.
46. Alper, H., and R. Levy. 1989. Computer simulations of the dielectric properties of water: studies of the simple point charge and transferable intermolecular potential models. *J. Chem. Phys.* 91:1242–1251.
47. Jayarm, B., R. Fine, K. Sharp, and B. Honig. 1990. Free energy calculations of ion hydration: an analysis of the Born model in terms of microscopic simulations. *J. Phys. Chem.* 93:4320–4327.
48. Diamond, R. 1990. On the use of normal modes in thermal parameter refinement: theory and application to the bovine pancreatic trypsin inhibitor. *Acta Crystollogr.* A46:425–435.
49. Warshel, A., and F. Sussman. 1985. Calculation of electrostatic energies in proteins. The energetics of ionized groups inbovine pancreatic trypsin inhibitor. *J. Mol. Biol.* 185:389–404.
50. Mérola, F., R. Rigler, A. Holmgren, and J. C. Brochon. 1989. Picosecond tryptophan fluorescence of thioredoxin: evidence for discrete species in slow exchange. *Biochemistry.* 28:3383–3398.
51. Hol, W. 1985. The role of the α helix dipole in protein function and structure. *Prog. Biophys. Mol. Biol.* 45:149–195.
52. Wada, A. 1977. The α helix as an electric macrodipole. *Adv. Biophys.* 9:1–63.